CURIOSIS

APPLICATION NOTE

Cellular assay using brightfield and fluorescence-based live cell imaging

Using Celloger series to image cells in real time

Live cell imaging technique makes it possible to understand and study various biological phenomena by enabling the observation of complex dynamics of live cells in real time using time-lapse microscopy. Real-time imaging of cellular phenomena such as cell migration, development and trafficking serves as an important means for research in various academic fields including cell biology, neuroscience, pharmacology and developmental biology. In order to observe the cells in a live state, incubator function is added to cover the microscope to control carbon dioxide, temperature and humidity (Figure 1A). But in many cases, controlling the temperature and humidity suitable for cell growth is challenging due to difficulties in maintaining airtightness and covering a large volume. To overcome such shortcomings, affordable and compact imaging devices that can be put into a cell culture incubator are being developed. Such live cell imaging devices basically provide bright-field images and at times come with fluorescence imaging functionality to observe fluorophores being excited and emitted in a specific wavelength. However, live cell imaging using fluorescence staining has a limitation since making fluorescence brighter and clearer not only results in improved image quality but inevitably causes cellular phototoxicity. Thus, it is essential for the time-lapse imaging system to enable efficient fluorescence imaging even at a low light intensity. As mentioned earlier, it is a crucial aspect for the live cell imaging system to ensure the image quality while maintaining temperature and humidity when processing experiments that generate significant amount of heat such as fluorescence imaging inside an incubator.

Celloger series, live cell imaging systems developed by Curiosis, are made in a compact size so that they can be placed in a general cell culture incubator (Figure 1B) and designed to endure the self-generated heat enabling the long-term imaging. In addition to that, it can obtain clear bright-field images using contrast-enhanced optics and fluorescence images of live cells in real time with a minimum light intensity by optimizing fluorescence filter and light path. The systems were tested to verify the applications in various cell-based research on the fields such as cell biology and pharmacology. The results showed that the devices had higher bright-field image quality than other live cell imaging system with the same functions and fluorescence imaging results were comparable to the images obtained from fluorescence microscopy using cMOS cameras with specifications corresponding to that of **Celloger.**

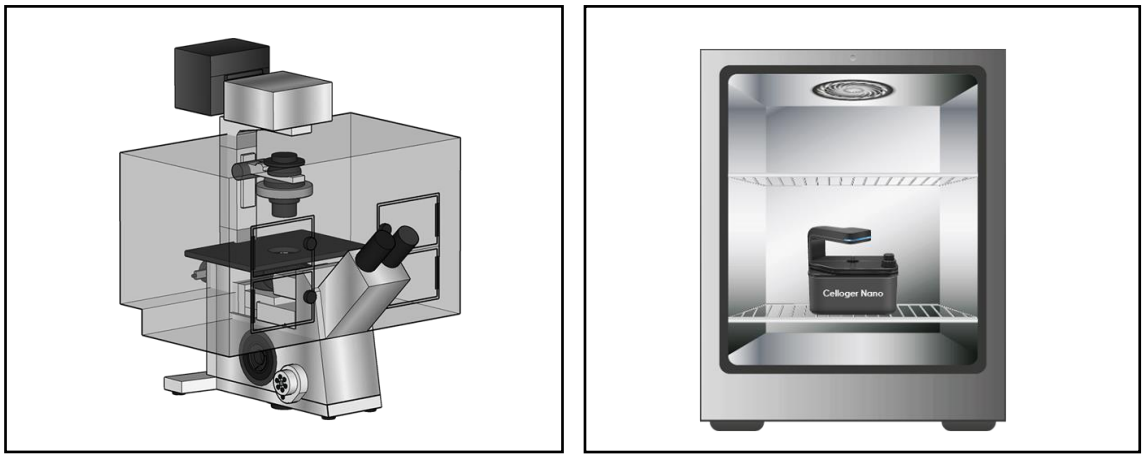

A. Conventional microscope

B. Celloger Nano placed in an incubator

Figure 1. Live cell imaging systems

1. Bright-field imaging application

Drug screening is a very important and essential process for the development of drugs including anticancer drugs. For drug screening, it is important to obtain a clear image in the process of real-time cell monitoring while performing treatment according to the type or concentration of a drug. **Celloger**'s bright-field imaging has increased the contrast in comparison to the existing live cell imaging equipment, making it possible to display more vivid cell contours and boundaries despite the usage of transparent cell samples (Figure 2).

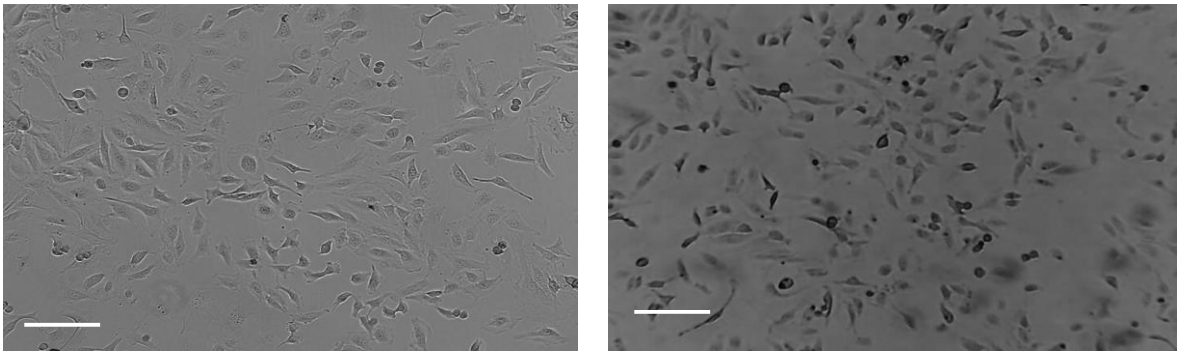

A. Image taken by Celloger Nano

B. Image taken by live cell imaging device of another company

Figure 2. Hela cell bright-field imaging (Scale bar, 200μm)

1.1. Morphology monitoring and drug screening

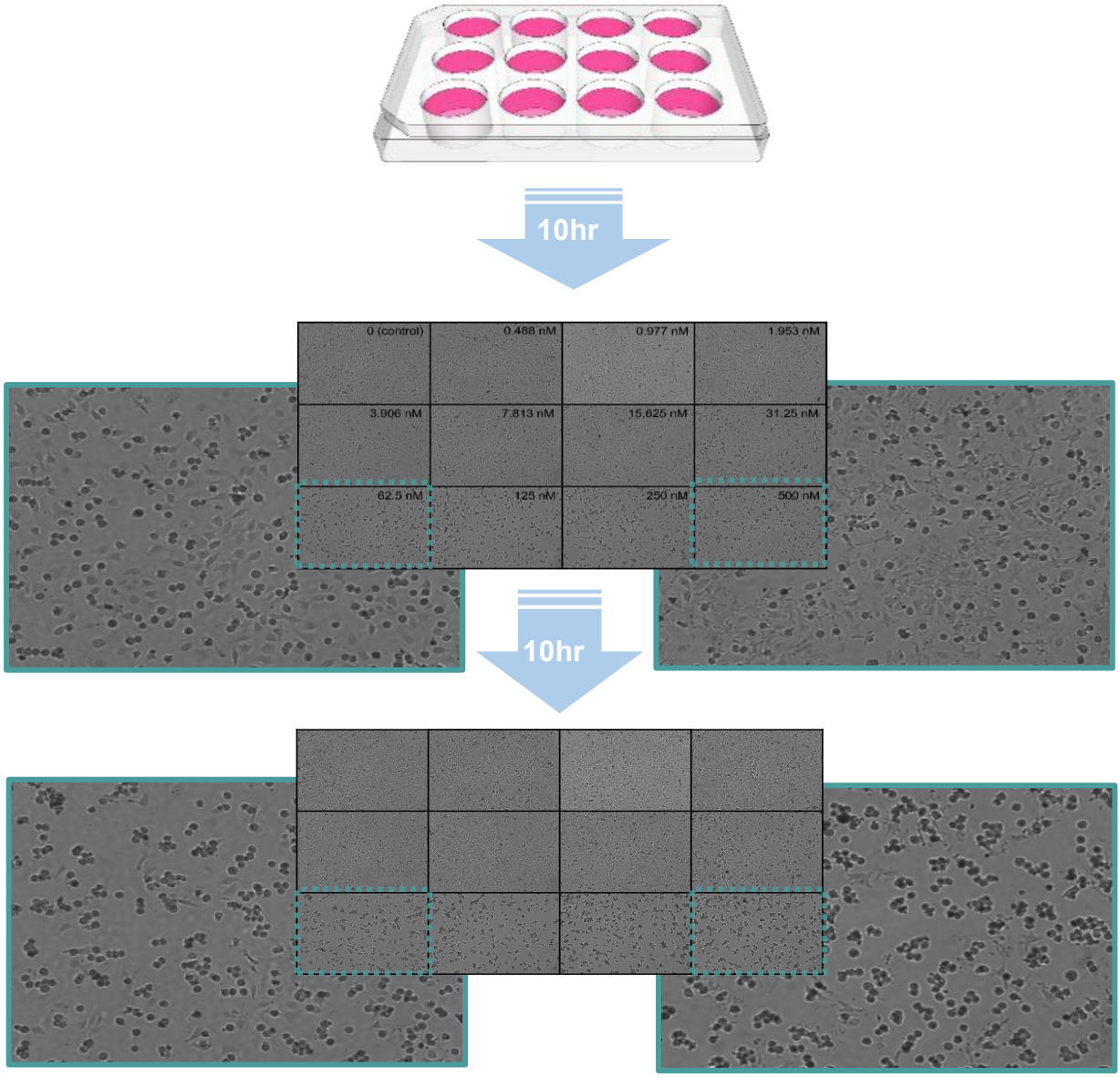

*The images were collected hourly by Celloger Mini for 20hrs.

Figure 3. Image tiles for different concentration levels of nocodazole and timelapse images generated by Celloger Mini.

With Celloger Mini, the designated positions of multiple points can be scanned according to a set schedule as it has automatic motorized stages. This feature makes it possible to track the changes over time when cells are treated with different drug concentrations. Nocodazole, one of the anticancer drugs, is known to cause mitotic arrest by inhibiting the polymerization which cell and what concentration it is used[1,2]. Cells were treated with different concentration levels of nocodazole and observed by **Celloger Mini**. The results showed that most cells died had similar confluency at the final endpoint, 20 hours after the treatment with the drug when the drug concentration is over 62.5nM. On the contrary, there was difference in cell death and confluency depending on concentration levels of the drug in early time.

As such, it was possible to obtain important data for morphological dynamics of cells and antitumor efficacy of drug through real-time cell monitoring and confluency imaging using **Celloger Mini.** As shown in Figure 3, time-lapse images are generated in tile images, making it easy to compare the differences depending on conditions.

2. Fluorescence imaging application

Using live cell imaging equipment such as **Celloger Nano**, it becomes possible to visually investigate the dynamics of intracellular changes using the live cell staining fluorescent dyes with specific staining properties for subcellular organelles and cell labelling. Using this characteristic, it is possible to monitor and quantify the efficacy of a drug through various mechanisms. Fluorescence optics of **Celloger Nano** were optimized to increase the ratio of detected fluorescence to light source intensity, resulting in improved fluorescence image quality while minimizing phototoxicitythat occurs inevitably during excitation. The fluorescence images taken by **Celloger Nano** were compared with those taken by a fluorescence microscope equipped with a ASI174MM camera (SONY IMX174 cMOS image sensor) whose specification is comparable to that of **Celloger Nano** to verify the quality of fluorescence images. The fluorescence image of Hela cells stained with fluorescence dye using CMFDA, a green fluorescent cell tracker, taken by **Celloger Nano** showed that the fluorescence intensity was comparable to that of fluorescence microscope and the image was clear since the contrast between the background and cells was high (Figure 4).

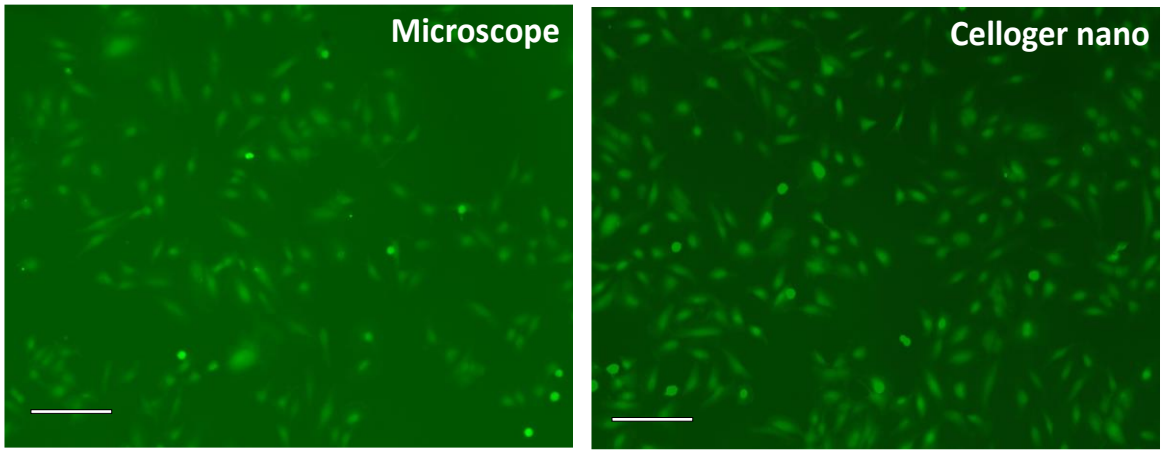

Figure 4. Fluorescence imaging of CMFDA stained cells (Scale bar, 200μm)

2.1. Cytotoxicity assay

Several staining reagents that measure the degree of cell death using a phenomenon in which the integrity of the cell membrane is damaged and the cell permeability is increased during the cell death are commercially available. To measure the cytotoxicity by nocodazole, dead cells were stained with green fluorescent CellTox™ dye. It was confirmed that the number of cells measured by fluorescence increased as the cell permeability increases due to cell death after 20 hours (Figure 5).

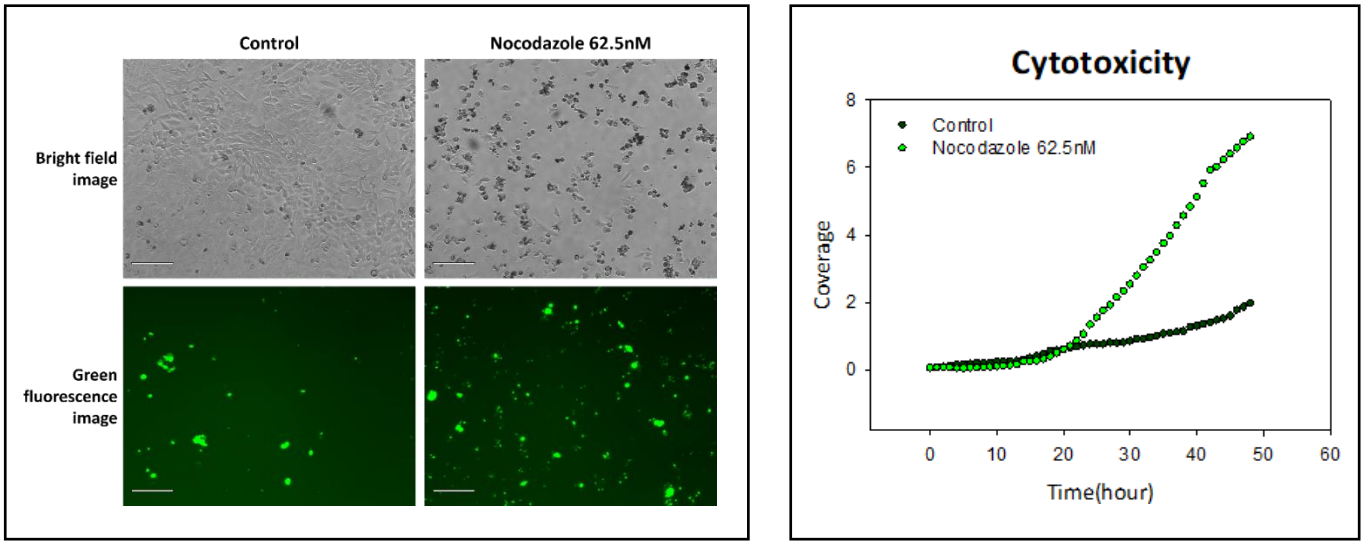

A. Cell image after 35 hours from the treatment with 62.5nM nocodazole. (Scale bar, 200um)

B. Fluorescence coverage by hour

Figure 5. Cytotoxicity assay using cell-impermeant dye

2.2 Apoptosis assay

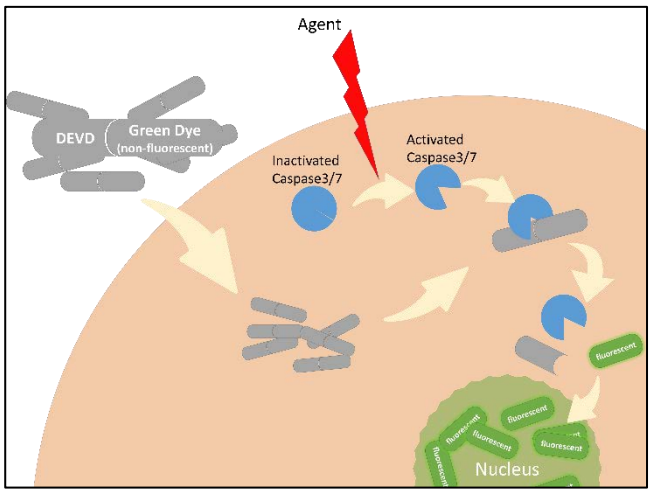

Figure 6. Illustration on the action mechanism of Caspase-3/7 Green Detection Reagent

Apoptosis is the process of programmed cell death where processes such as membrane blebbing, cell shrinkage and nuclear fragmentation occur. In this process, the enzyme called caspase is activated to mediate this reaction in the cell. Activated Caspase3/7, one of the caspase family, specifically cleave certain peptide known as DEVD, and fluorophores conjugated DEVD is useful to quantify Caspase activity and apoptosis (Figure 6).

It was found that fluorescent materials were released and detected after cleavage of DEVD caused by the treatment with staurosporine, a material known to activate caspase and cause apoptosis. The amount of fluorescent materials increased with time (Figure 7).

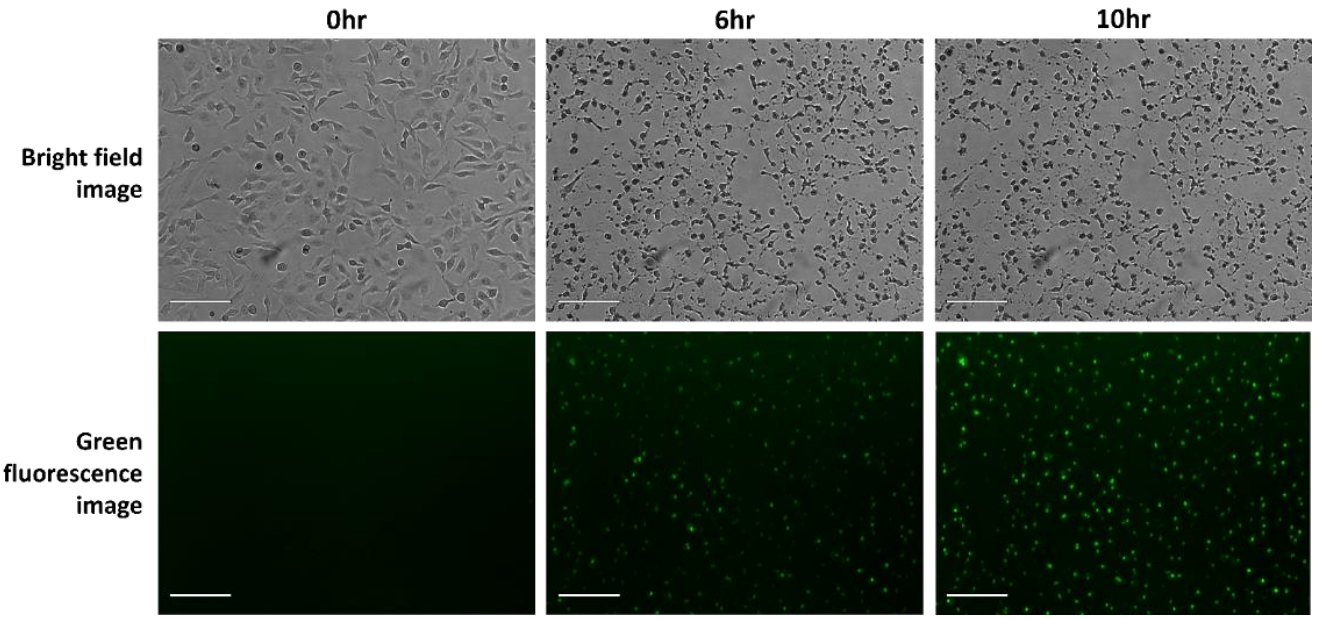

* The images were collected every 30min by Celloger Nano for 15hrs and 30mins.

Figure 7. Using fluorescence detection of activated caspase to quantify apoptosis of Hela cells caused by staurosporine (Scale bar, 200μm)

Fluorescence coverage graph is shown to quantify the apoptosis by time. The graph illustrates that fluorescence began to be detected from two and a half hours after the treatment with staurosporine and reaction became saturated from 10 hours after the treatment, making it possible to detect fluorescence in all cells (Figure 8).

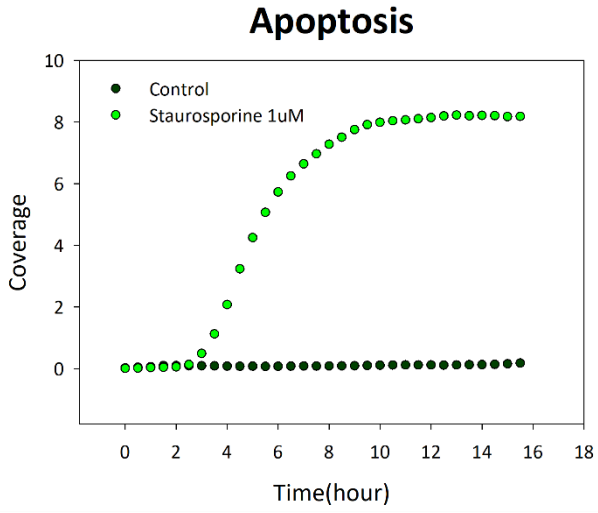

Figure 8. Fluorescence coverage graph by time

2.3 Transfection

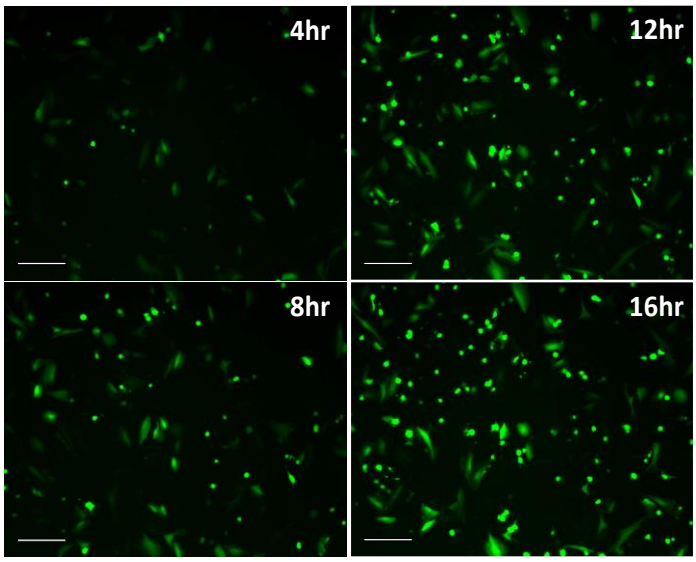

* The images were collected every 2hrs by Celloger Nano for 40hrs.

Figure 9. Time lapse image of EGFP expression following pCMV GFP plasmid Transfection (Scale bar, 200μm)

Gene transfection is conducted for various research and therapeutic purposes. Real-time cell imaging is considered to be used well in various applications for quantifying cell transfection efficiency or monitoring the effect of transfected genes. The fluorescence with the expression of green fluorescence protein in pCMV-GFP vector transfected in a cell was observed every 2 hours through **Celloger Nano** and it was confirmed that the green fluorescence protein started to be expressed from 4 hours after transfection and it was maintained strongly until 16 hours after transfection (Figure 9).

3. Conclusion

The **Celloger series** improves the efficiency of fluorescence imaging by enabling imaging even at a minimum level of excitation light, which can also reduce phototoxicity caused by fluorescence staining, a priority consideration for live cell imaging. The **Celloger systems** that were used to carry out the applications mentioned above work perfectly inside an incubator, which makes them ideal tools for various imaging applications and experiments.

4. Reference

1. Jordan, M. A., Thrower, D., & Wilson, L. (1992). Effects of vinblastine, podophyllotoxin and nocodazole on mitotic spindles. Implications for the role of microtubule dynamics in mitosis. *Journal of cell science*, *102* (1), 401-416.

2. Blajeski, A. L., Phan, V. A., Kottke, T. J., & Kaufmann, S. H. (2002). G 1 and G 2 cell-cycle arrest following microtubule depolymerization in human breast cancer cells. *The Journal of clinical investigation*, *110* (1), 91-99.

CURIOSIS

APPLICATION NOTE

Assessment of adipogenesis degree in real time

Using Celloger® Pro

■ Introduction

Adipocytes serve as crucial energy reservoirs, efficiently converting surplus calories into fat for future energy needs. However, excessive fat accumulation can lead to obesity, a condition associated with various health problems in our modern society.[1] Beyond their role in metabolism, adipocytes also influence immune responses and reproductive functions[2] through hormone utilization such as leptin and adiponectin.

The process of adipogenesis, where preadipocytes differentiate into mature adipocytes, varies across species. Additionally, the proportion of cells undergoing adipogenesis differs between in vivo tissues and in vitro cell culture plates.[3] Researchers actively investigate the factors involved in adipogenesis and the intricate regulatory mechanisms underlying this complex process.

In a review conducted by Sylvia P. Poulos, the differentiation ratio of cells varies depending on the components of the culture media. Additionally, the expression levels of transcription factors associated with adipogenesis change over time, whether during seeding or post-confluence. Therefore, assessing the degree of adipogenesis at different time points is crucial. The use of automated live-cell imaging equipment, such as the Celloger® Pro, makes it convenient to monitor and measure adipogenesis. In this application note, we introduce methods for assessing adipogenesis during the differentiation process using the widely studied preadipocyte cell line, 3T3-L1.

■ Materials and Methods

Cell maintenance and cell confluency inspection

3T3-L1 cells were cultured in DMEM (Dulbecco's Modified Eagle's Medium with high glucose, Welgene, LM001-10) supplemented with 10% BCS (Bovine Serum, Gibco, 26170043) and 1% P/S (Penicillin-Streptomycin, Gibco, 15140122). When the cells reached 80~90% confluence, they were sub-cultured. To induce differentiation, cells were seeded in a 12-well plate at concentrations of $1X10^4$ cells/cm^2, $5X10^3$ cells/cm^2, $2.5X10^3$ cells/cm^2, and $1.25X10^3$ cells/cm^2. After seeding, the culture medium was changed on the second day, and then on the following day, the cell density was measured using the Celloger® Pro with a 4X lens.

Adipogenesis induction using differentiation media (DM) and observation of cell morphology during adipogenesis

On the second day after achieving confluency, we introduced DM I, which consists of DMEM supplemented with 10% FBS (Fetal Bovine Serum, Welgene, S001-01), 1% P/S, 1 μg/ml Insulin (Insulin solution human, Sigma, I9278-5ML), 0.25 μM Dexamethasone (Sigma, D2915-100MG), and 0.5 mM IBMX (3-Isobutyl-1-methylxanthine, Sigma, I5879-100MG). After an additional two days of cultivation, we switched to DM II, composed of DMEM supplemented with 10% FBS, 1% P/S, and 1 μg/ml Insulin. To assess the impact of Rosiglitazone on adipogenesis, we added 2 μM Rosiglitazone (Sigma, R2408-10MG) to both DM I and DM II. Throughout the differentiation period, cell images were captured at one-hour intervals using the Celloger® Pro equipped with 4X or 10X lenses.

Quantification of lipid droplet using fluorescence

During the differentiation process, cells were cultured with 1 μM LipiDye II (FDV-0027, Funakoshi) to fluorescently observe lipid droplets. The coverage (%) of green fluorescence was measured using the Celloger analysis software to calculate the area of the lipid droplets. To enhance the accuracy of assessing the uneven occurrence of adipogenesis, five randomly selected points per well were imaged, and the average value was calculated.

■ Result

Observing morphological changes during differentiation

The most significant structural change during adipocyte differentiation is the formation of lipid droplets. These are organelles enveloped by a monolayer of phospholipids, containing triglycerides and sterol esters. Adipocytes are classified into brown, beige, and white cells, each with unique characteristics. Unlike beige and brown cells, which typically contain multiple lipid droplets per cell, white cells are characterized by a single, large lipid droplet that occupies a significant portion of the cytoplasm, making them easily distinguishable from other cell types (Figure 1).

These three types of adipocytes have distinct functions. White adipose tissue (WAT), prevalent in obesity, primarily serves as an energy storage site, while brown adipose tissue (BAT) aids in energy expenditure through thermogenesis. Recent studies have highlighted that Batokines, factors released by BAT, can impact various organs[4], thereby influencing overall metabolism.[4, 5] Additionally, beige fat cells, situated within WAT, exhibit traits similar to those of BAT, including thermogenic capabilities. Moreover, these cells can undergo transdifferentiation from mature WAT[6], attracting significant attention from many researchers.

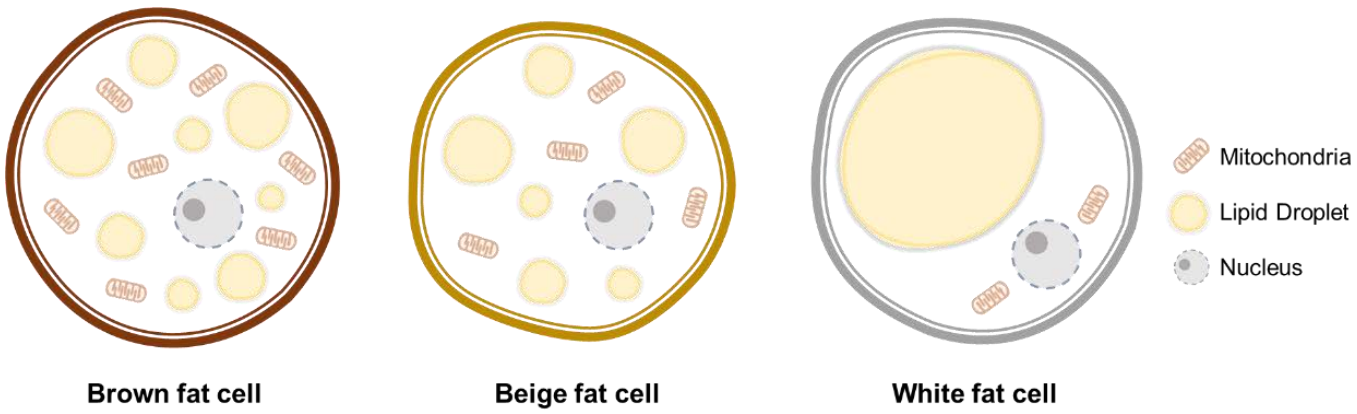

Figure 1. Three types of adipocytes

We induced adipogenesis in 3T3-L1 cells and observed changes in cell morphology at one-hour intervals throughout the process using the Celloger® Pro. Figure 2 depicts the differentiation process of 3T3-L1 cells over time. While the timing of lipid droplet formation varied depending on cell passage, in most cases, it was promptly observed following the introduction of DM II containing Rosiglitazone. The cells predominantly evolved into brown fat-like cells with numerous tiny lipid droplets. Using the Celloger® Pro with a 10X lens, we could distinctly identify lipid droplets over 3 μm in diameter as clear, water droplet-shaped figures, eliminating the need for further staining.

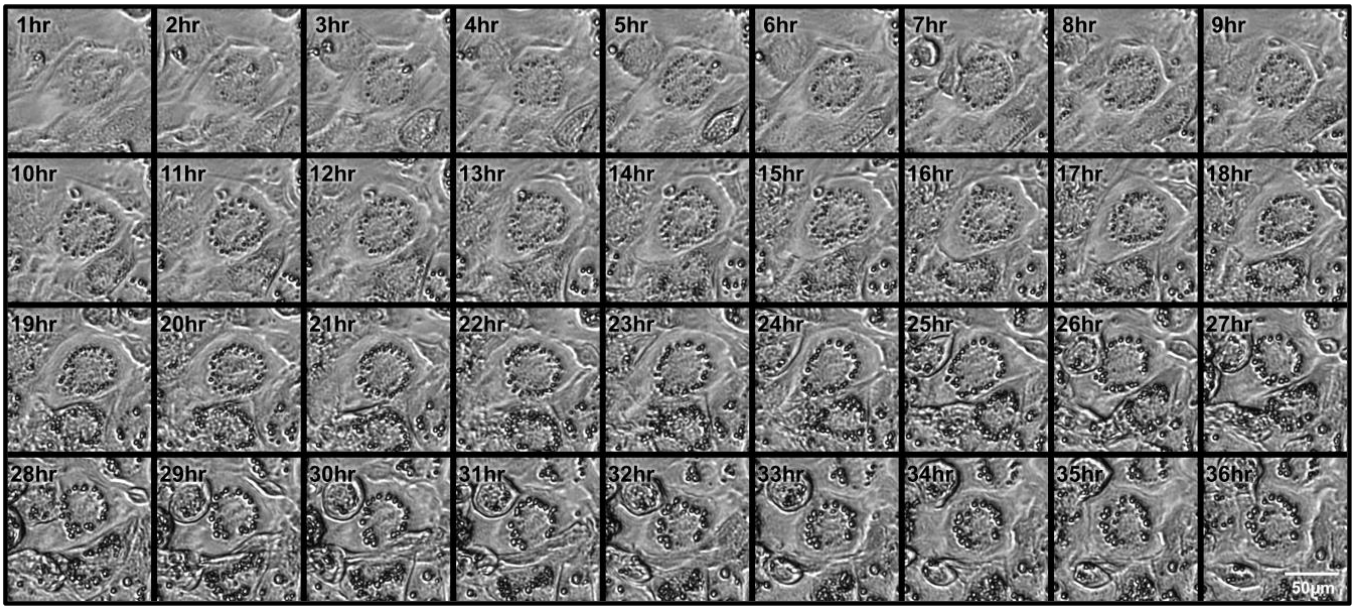

Figure 2. Time-lapse sequence of adipocytes during differentiation

This sequence presents images captured at one-hour intervals from 1 hour to 36 hours after treatment with DM II and Rosiglitazone. (using a 10X magnification, cropped images)

Quantification of lipid droplet in real time

Many researchers use Oil Red O reagent to assess the level of differentiation by evaluating the extent of lipid droplets. Oil Red O is a dye commonly used to stain lipid-rich structures such as lipid droplets, enabling visualization under a microscope. However, staining is not feasible under physiological conditions, making it difficult to track changes over time. Therefore, we chose LipiDyeII, a fluorescent dye suitable for live cells. LipiDyeII not only stains lipid droplets but also allows for analysis in live cells, making the process straightforward. Cells in DM containing LipiDyeII exhibited a gradual manifestation of lipid droplets, characterized by green fluorescence. The fluorescent signals precisely coincide with the enveloped structures observed in the bright field image (Figure 3). Even when lipid droplets are obscured within cell structures (indicated by arrows in Figure 3) or are too small to distinguish in bright field (depicted by the dotted circle in Figure 3), they can be readily identified using fluorescence.

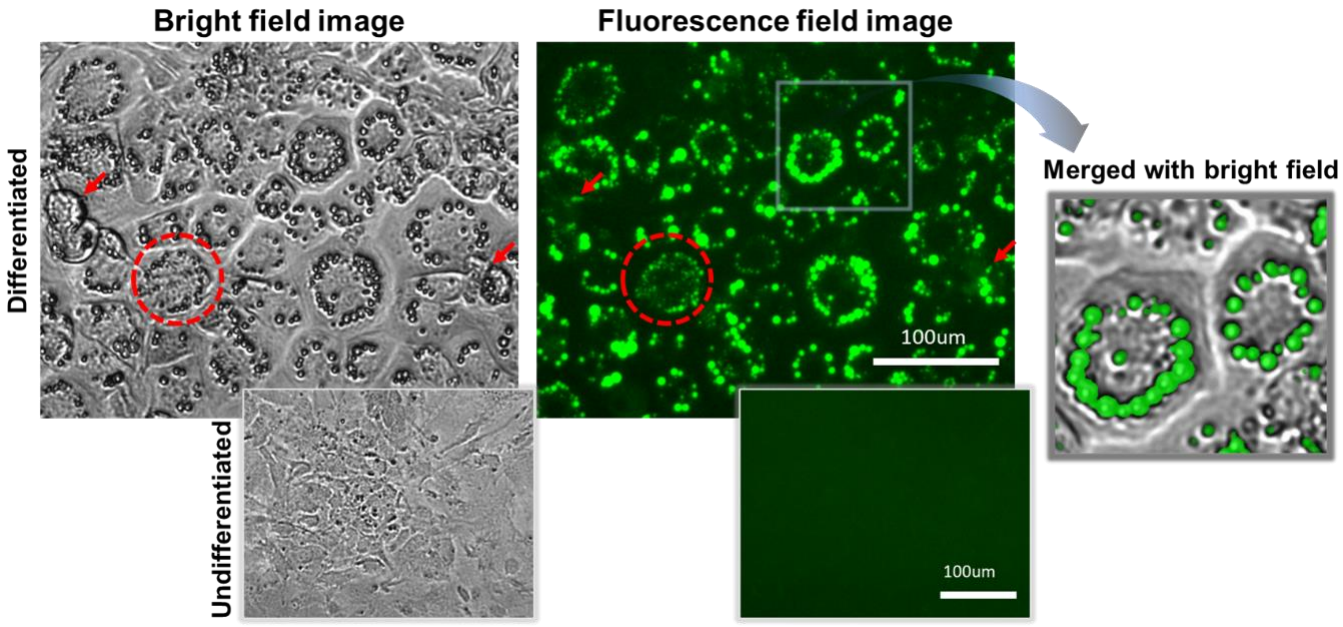

Figure 3. Observation of adipocyte with lipid droplet in bright field and fluorescence field

Images were captured 24 hours after replacing DM II containing Rosiglitazone and treating with LipiDyeII using Celloger® Pro with a 10X lens.

We quantified the differentiation ratio by measuring the fluorescence coverage, which indicates the proportion occupied by lipid droplets (Figure 4). Since differentiation does not occur uniformly across the entire plate but rather in patches, it is necessary to examine a wide area for comprehensive analysis. However, using low magnifications such as 2X is insufficient for accurately measuring small lipid droplets. Therefore, by utilizing a 4X magnification and the multi-position imaging function to scan multiple points, we were able to measure the proportion of lipid droplets over a slightly wider range and obtain more reliable data.

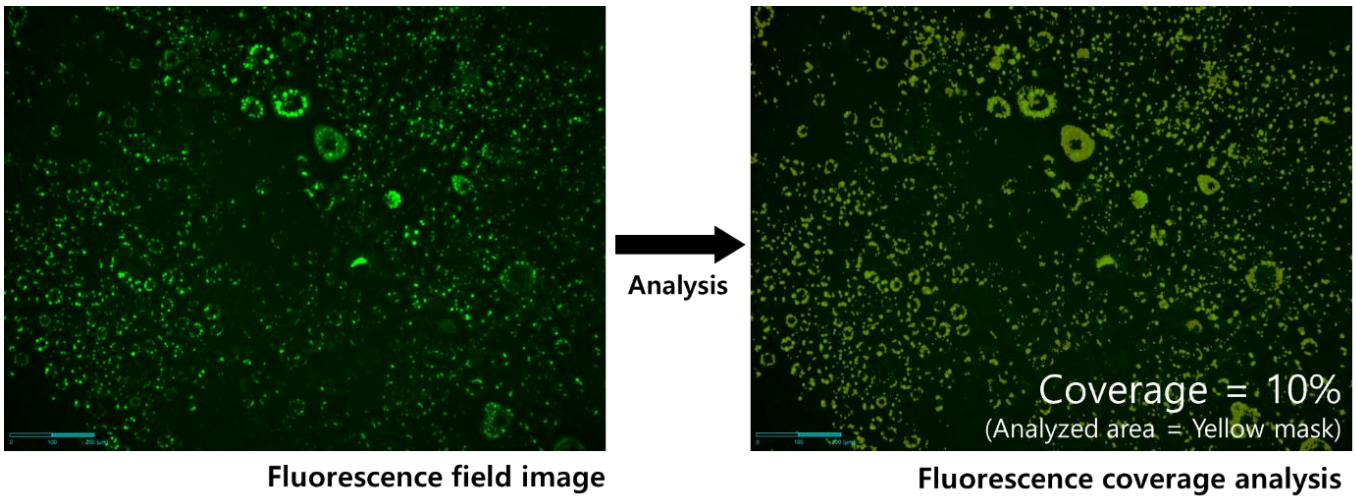

Figure 4. Measurement of lipid droplet area using Celloger analysis software

The image was captured using the Celloger® Pro with a 4X lens on the second day after treatment with DM II and LipiDyeII. Fluorescence area was distinguished using the **adaptive threshold method* and calculated in the Celloger analysis software.

**Adaptive threshold method: an image processing technique that calculates varying threshold values for different regions of an image based on local pixel value, enabling effective segmentation in images with uneven illumination or contrast.*

Assessment of differentiation level based on cell density and the Rosiglitazone administration

The adipocyte differentiation process is highly regulated and influenced by numerous factors, including the preadipocytes' environment and pharmacological interventions.[7, 8, 9] Among these, cell confluency at the time of induction of differentiation is recognized as a crucial parameter that affects the efficiency and quality of adipocyte formation.[10] Furthermore, pharmacological agents such as Rosiglitazone, a potent agonist of peroxisome proliferator-activated receptor gamma (PPARγ), have been demonstrated to play a vital role in modulating adipogenesis.[11, 12, 13, 14, 15] PPARγ is a key transcription factor that drives the expression of various genes involved in adipocyte maturation and function.

To understand the interplay between cell confluency and Rosiglitazone treatment in the context of adipocyte differentiation, we evaluated the degree of differentiation following the experimental scheme as described in Figure 5.

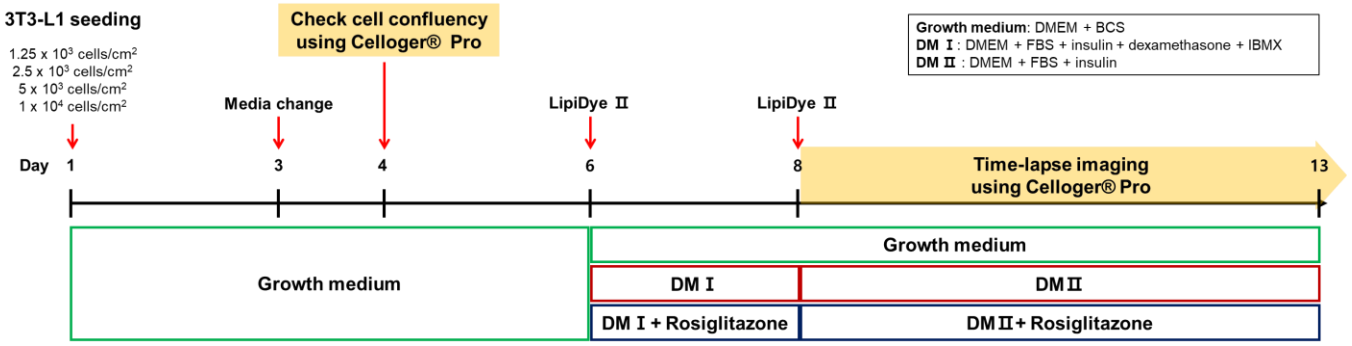

Figure 5. Experimental scheme of 3T3-L1 differentiation

To evaluate how the initial density of cells affects the differentiation of adipocytes, we seeded 3T3-L1 cells at four different densities. On the third day post-seeding, we acquired cell images to verify the level of confluency using Celloger's reservation functions, which automatically captured cell images on the designated date (Figure 6a). These captured images were then analyzed using Celloger analysis software to determine the degree of confluency (Figure 6b). This initial assessment was critical to establish a baseline for understanding the influence of cell confluency on subsequent differentiation.

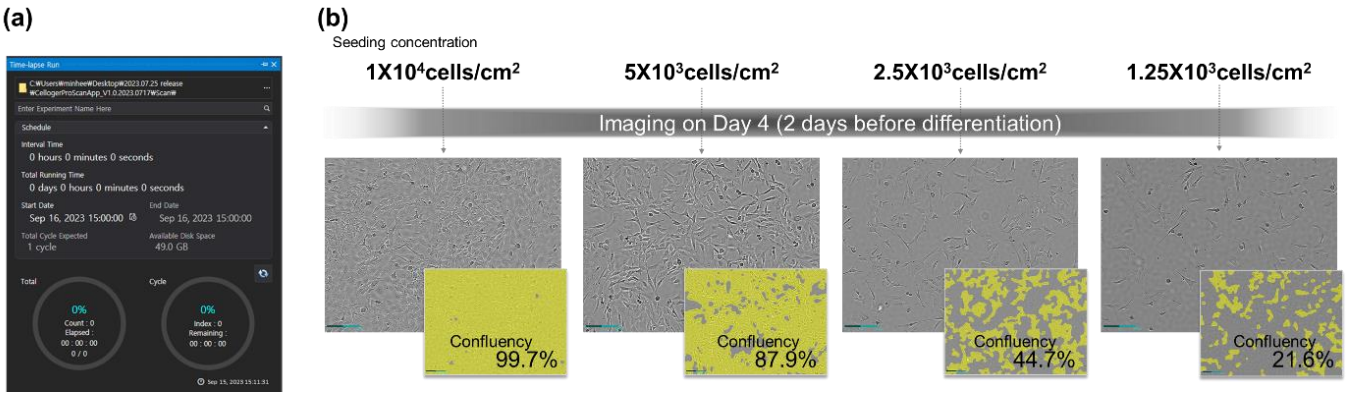

Figure 6. Confirmation of cell confluency according to cell seeding density

After seeding the cells, we assessed their confluency on the third day using Celloger's time-lapse scheduling feature. (a) Celloger scan software time-lapse schedule window (b) Images analyzing cell confluency

On day 6, two days after verifying cell confluency, we initiated the adipocyte differentiation process. To determine the impact of Rosiglitazone on this process, experiments were conducted with two groups: one treated with DM containing Rosiglitazone and the other without Rosiglitazone (Figure 5). We assessed the adipocytes' differentiation level by applying LipiDyeII dye and then measuring the fluorescent coverage, which indicates the lipid droplet area. This measurement was conducted at five different positions using the Celloger analysis software. Figure 7 presents the results observed on the day 13 (Figure 7a) and over the entire 5-day period (from day 8 to day 13) (Figure 7b) after addition of DM II with or without Rosiglitazone. The administration of Rosiglitazone markedly augmented the rate of adipocyte differentiation, as indicated by the enhanced fluorescence area denoting increased lipid accumulation. Cells maintained in DM II without Rosiglitazone manifested a differentiation rate of merely 4.7% after 120 hours. Conversely, culturing cells in DM II with Rosiglitazone led to a rapid increase in differentiation, reaching a cell differentiation percentage of 16.6% within 97 hours. However, there was little difference in the degree of differentiation based on cell concentration.

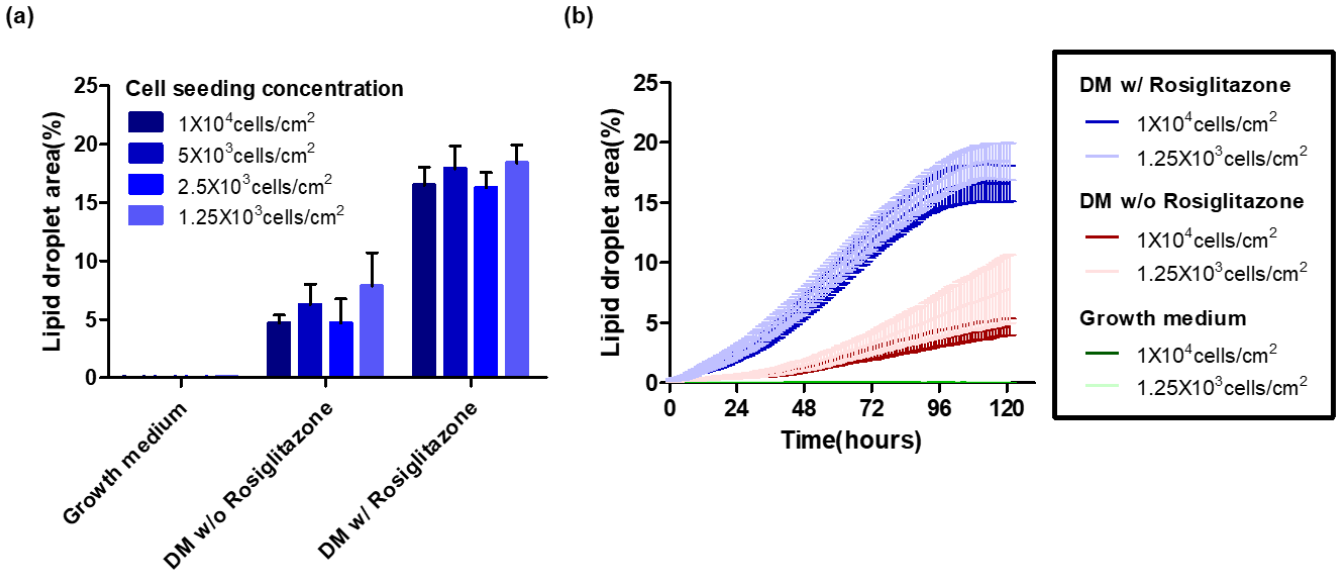

Figure 7. Quantification of lipid droplet area depending on cell density and the Rosiglitazone administration

(a) The bar graph illustrates the degree of adipogenesis depending on cell density on day 13. Error bars represent the standard error (n=5). (b) This graph shows the progression of lipid droplet formation over time after the addition of DM II (from day 8 to day 13). The analysis involved capturing fluorescent images at five different locations, with standard errors depicted by shaded areas in pink or sky-blue (DM w/ Rosiglitazone: n=5, DM w/o Rosiglitazone: n=5, Growth medium: n=1). Cells treated with DM II containing Rosiglitazone exhibited a significantly faster increase in differentiation compared to those without Rosiglitazone, as indicated by a two-tailed t-test with a p-value < 0.0001. The growth medium group represents cells that were not subjected to DM treatment. To prevent graph complexity, other concentrations were omitted.

■ Conclusion

Adipogenesis is a complex process regulated by the expression levels of various factors, often temporally controlled or influenced by interactions with other cellular elements. Understanding these intricate mechanisms necessitate meticulous observation over extended periods. Traditionally, researchers have assessed the expression levels of specific markers at certain time points during differentiation. However, the Celloger® Pro system has revolutionized this approach by allowing continuous, long-term monitoring of these pathways. With its time-lapse scheduling feature, researchers can conduct prolonged observations without time constraints, thereby enhancing experimental efficiency. A notable feature of Celloger® Pro is its adjustable magnification levels, enabling high-magnification observation of lipid droplet formation, while lower magnifications capture a broader image area to evaluate overall adipocyte differentiation. Additionally, by fluorescently staining lipid droplets and utilizing Celloger's analysis software to measure fluorescence intensity, researchers can quantify the degree of differentiation, providing numerical values to the observed changes. This combination of features offers invaluable insights into the dynamic regulatory mechanisms governing adipocyte differentiation, advancing our understanding of adipogenesis and its critical role in metabolic health.

Reference

1. Lennarz, William J., and M. Daniel Lane. "Adipogenesis" Encyclopedia of biological chemistry. Academic Press, 2013. 52-56

2. Britannica, The Editors of Encyclopaedia. "adipose cell". Encyclopedia Britannica, 18 May. 2020, https://www.britannica.com/science/adipose-cell. Accessed 28 November 2023.

3. Poulos, Sylvia P., Michael V. Dodson, and Gary J. Hausman. "Cell line models for differentiation: preadipocytes and adipocytes." Experimental biology and medicine 235.10 (2010): 1185-1193.

4. Yang, Felix T., and Kristin I. Stanford. "Batokines: mediators of inter-tissue communication (a mini-review)." Current Obesity Reports 11.1 (2022): 1-9.

5. Ahmad, Bilal, et al. "Brown/Beige adipose tissues and the emerging role of their secretory factors in improving metabolic health: The batokines." Biochimie 184 (2021): 26-39.

6. Cinti, Saverio. "Reversible physiological transdifferentiation in the adipose organ: symposium on 'frontiers in adipose tissue biology'." Proceedings of the Nutrition Society 68.4 (2009): 340-349.

7. Benchamana, Ameena, et al. "Regulation of adipocyte differentiation and metabolism by lansoprazole." Life sciences 239 (2019): 116897.

8. Pu, Yong, and Almudena Veiga-Lopez. "PPARγ agonist through the terminal differentiation phase is essential for adipogenic differentiation of fetal ovine preadipocytes." Cellular & Molecular Biology Letters 22 (2017): 1-12.

9. Teixeira, Catarina, et al. "Enhanced 3T3-L1 differentiation into adipocytes by pioglitazone pharmacological activation of peroxisome proliferator activated receptor-gamma (PPAR-γ)." Biology 11.6 (2022): 806.

10. Cornelius, Peter, Ormond A. MacDougald, and M. Daniel Lane. "Regulation of adipocyte development." Annual review of nutrition 14.1 (1994): 99-129.

11. Farmer, S. R. "Regulation of PPARγ activity during adipogenesis." International journal of obesity 29.1 (2005): S13-S16.

12. Wabitsch, Martin, et al. "Characterization of a human preadipocyte cell strain with high capacity for adipose differentiation." International journal of obesity 25.1 (2001): 8-15.

13. Tontonoz, Peter, et al. "Terminal differentiation of human liposarcoma cells induced by ligands for peroxisome proliferator-activated receptor γ and the retinoid X receptor." Proceedings of the National Academy of Sciences 94.1 (1997): 237-241.

14. Zebisch, Katja, et al. "Protocol for effective differentiation of 3T3-L1 cells to adipocytes." Analytical biochemistry 425.1 (2012): 88-90.

15. Zhao, Xueyan, et al. "A comparison of methods for effective differentiation of the frozen-thawed 3T3-L1 cells." Analytical biochemistry 568 (2019): 57-64.

CURIOSIS

APPLICATION NOTE

Quantification of mitochondrial membrane potential

Using Celloger® Pro

■ Introduction

Mitochondria serve as the primary organelles responsible for generating energy within cells. In particular, Mitochondrial Membrane Potential (MMP) is considered a key indicator of mitochondrial function, as it is vital for ATP production.[1] Hence, MMP measurement has long been used as a marker for evaluating apoptosis, cell viability, and overall cellular health. Moreover, given that mitochondrial function is recognized to play a crucial role in conditions such as cancer, diabetes, and brain disorders like Alzheimer's and Parkinson's diseases[2], understanding and monitoring MMP become more significant.

Today, numerous fluorescent probes have been developed to visualize mitochondrial potential, including TMRE, TMRM, JC-1, JC-10, Mito-ID, MitoTracker and so on. Among these, JC-1 and JC-10 dyes exhibit changes in fluorescence wavelength depending on the probe's form. In healthy cells with normal MMP, JC-10 accumulates within the mitochondria, forming aggregates that emit red fluorescent wavelengths. On the other hand, in unhealthy cells with declined MMP, such as apoptotic cells, JC-10 scatters across the cytoplasm and converts into monomers, emitting green fluorescent wavelengths.[3] In this application note, we introduce a procedure for evaluating mitochondrial membrane potential using Celloger® Pro.

■ Method

HeLa cells were seeded at a density of 3.5 x 10^4 cells per well in a 24-well plate. Following overnight incubation, the cells were treated with carbonyl cyanide 3-chlorophenylhydrazone (CCCP) (Sigma, C2759-100MG) at concentrations of 0.5, 1, 2, 4, 6, 8, 10 and 20 μM for 20 minutes. After a wash with HBSS buffer, the cells were stained with 10 μM JC-10 (AAT bioquest, 22204) solution in the dark for an hour. Finally, images were taken with Celloger® Pro, automated live cell imaging system with a 2X lens.

■ Result

We observed changes in fluorescence resulting from depolarization using JC-10 dye and carbonyl cyanide 3-chlorophenylhydrazone (CCCP), which acts as an uncoupler of oxidative phosphorylation. For quantitative comparison, we captured green and red fluorescence images using the Celloger® Pro with 2X lens for a wide field-of-view. And then, we employed analysis software to measure the intensity changes. As the concentration of CCCP increased, the membrane potential depolarized, leading to a decrease in red intensity and an increase in green intensity. (Fig. 1A). This trend persisted until a concentration of 20 μM was reached, at which point red intensity became almost negligible, causing the cells to appear entirely green. Figure 1B, captured with the Celloger® Pro using a 2X lens and cropped for magnification, enables the observation of red and green fluorescence distribution. The graph in Figure 1C, which depicts the green/red intensity ratio in relation to CCCP concentration as a dot plot, showed a gradual ascending pattern suitable for polynomial regression curve fitting.

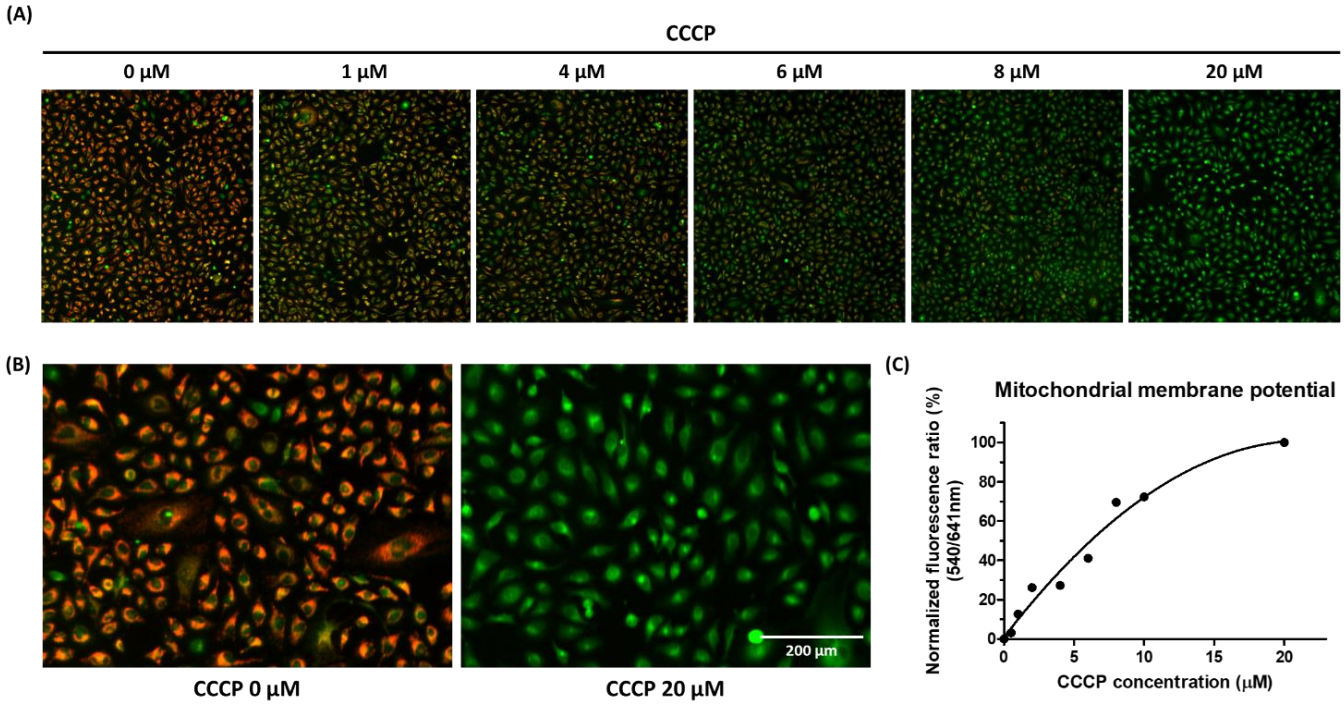

Figure 1. Mitochondrial dysfunction depending on CCCP concentrations.

(A) The intensity of both green and red fluorescence varied with different CCCP concentrations. (B) In the control group, strong red dot-like signals were observed, whereas CCCP-treated cells displayed a prominent spread of green fluorescence throughout the cytoplasm. (C) The relationship between the green/red ratio and CCCP concentrations is modeled using a second-order polynomial curve (R^2=0.97).

■ Conclusion

Mitochondrial activity in cells is intricately regulated in response to intracellular conditions, including factors such as MMP, which can vary depending on the stage of the cell cycle.[4] Therefore, it is important to analyze it within sufficiently wide areas to consider these variations, but collecting images from multiple regions is such a laborious task. Additionally, dyes like JC-10, which display two colors depending on their molecular forms, require individual detection using two different fluorescence channels. We successfully addressed these challenges by utilizing the Celloger® Pro, which offers features such as dual color fluorescence and bright-field imaging. Moreover, it efficiently captures images from multiple positions by automatically moving the camera.

Reference

1. Zorova, Ljubava D., et al. "Mitochondrial membrane potential." Analytical biochemistry 552 (2018): 50-59.

2. Bazhin, Arkadiy A., et al. "A bioluminescent probe for longitudinal monitoring of mitochondrial membrane potential." Nature chemical biology 16.12 (2020): 1385-1393.

3. Sivandzade, Farzane, Aditya Bhalerao, and Luca Cucullo. "Analysis of the mitochondrial membrane potential using the cationic JC-1 dye as a sensitive fluorescent probe." Bio-protocol 9.1 (2019): e3128-e3128.

4. Hirusaki, Kotoe, et al. "Temporal depolarization of mitochondria during M phase." Scientific Reports 7.1 (2017): 16044.

CURIOSIS

APPLICATION NOTE

Observation of dynamic changes in actin filaments during cell division

Using Celloger® Pro

■ Introduction

Cytokinesis is the final stage in cell division, during which the cytoplasm of one cell is physically divided into two separate cells. Actin filaments play a crucial role in supporting cell structure and facilitating division. Just before cell separation, actin filaments constrict the cell membrane, leading to the formation of two daughter cells.[1]

Cytochalasin B, a compound widely used in cell division and movement research, significantly affects the structure and dynamics of actin filaments. It primarily hinders cytokinesis by blocking the formation of contractile microfilaments. Interestingly, cytochalasin B exhibits distinct effects on cell behavior when employed at different concentrations, despite being the same drug. In high concentration of cytochalasin B induced a transformation in cell morphology, including contraction of actin cables, rounding up of fibroblastic cells.[2] However, low concentrations of cytochalasin B inhibited cell migration and membrane ruffling without causing any significant alterations in gross morphology.[3] Additionally, previous studies have shown that cytochalasin B can lead to incomplete cell division, resulting in the formation of multinucleated cells.[4] In this application note, we aim to demonstrate dynamic changes in cell structure upon cytochalasin B treatment using Celloger® Pro.

■ Method

HeLa cells stably expressing tdTomato-tagged actin were seeded in a 24-well plate at a density of $2.5x10^4$ cells per well. After overnight incubation, the cells were treated with cytochalasin B at concentrations of 1.25 μM (low-concentration) and 10 μM (high-concentration). Imaging was performed using the Celloger® Pro with a 10X lens at 1-hour intervals for 48 hours. Finally, cell nuclei were stained with 1 μM of SYTO9 (Invitrogen, S34854) for all groups except the high-concentration group.

■ Result

To understand the dynamic changes and structural characteristics of actin filaments induced by cytochalasin B during cell division, we used HeLa cell line stably expressing tdTomato-tagged actin and observed it in real-time over 48 hours. The images were captured using Celloger® Pro with a 10X lens and were cropped for analysis. In the control group, cells were divided from two cells to four daughter cells, undergoing a normal cell division (Fig. 1. Top panels). Conversely, cells treated with a low concentration of cytochalasin B failed to complete cell membrane separation, leading to the formation of multiple nuclei within a single cell (Fig. 1. Middle panels). However, cells treated with high concentrations of cytochalasin B exhibited severe disruption in actin filament structures, leading to irreversible cell rounding. (Fig. 1. Bottom panels). Quantitatively, a higher ratio of multinucleated cells is observed in the low-concentration of cytochalasin B-treated group compared to the control group (Fig. 2).

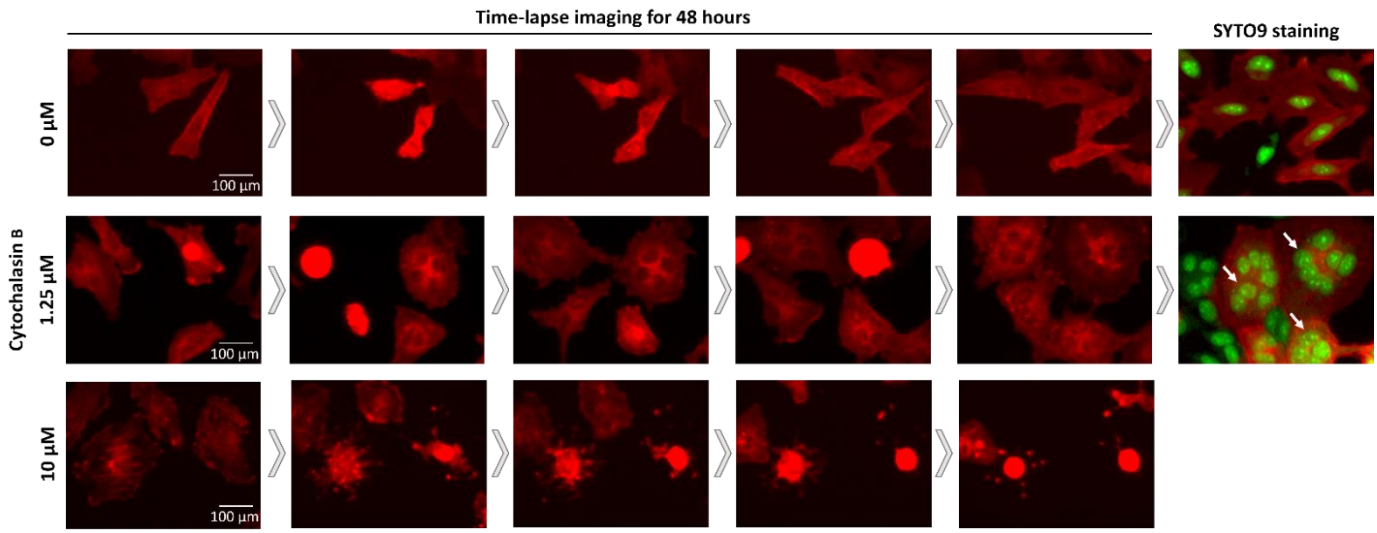

Figure 1. Visualization of dynamic changes in actin with various concentrations of cytochalasin B treatment.

HeLa cells treated with cytochalasin B at concentrations of 0 μM (control, top panels), 1.25 μM (low-concentration, middle panels) and 10 μM (high-concentration, bottom panels). Cells were imaged using a Celloger® Pro with a 10X lens, captured at 1-hour intervals. After 48 hours, cell nuclei were stained with 1 μM of SYTO9 except for the high-concentration group. (right panels).

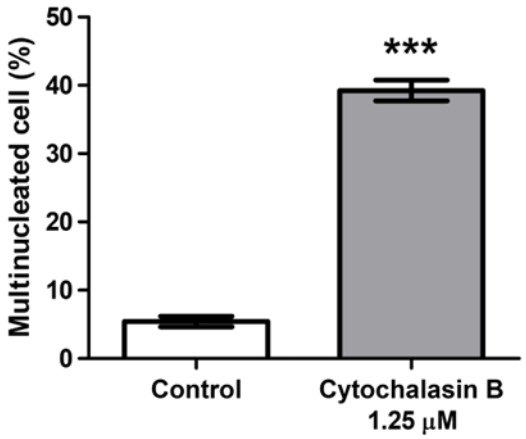

Figure 2. Low concentration of cytochalasin B treatment induced multi-nucleated cells.

The number of total cells and cells with two or more nuclei were counted at 9 random spots in the control (n=564) and cytochalasin B-treated (n=493) groups, respectively. The ratio of multinucleated cells was calculated as multi-nucleated cell/total cell. ***P <0.001.

■ Conclusion

Actin filaments within cells play a crucial role not only in cellular structure but also in the processes of cell replication and division. Real-time live imaging is essential for monitoring various cellular motility and responses to the drugs such as cytochalasin B, known for inhibiting actin filament formation. Particularly, when dealing with drugs that exhibit different reactions at various concentrations, obtaining diverse images for each concentration can be labor-intensive. In this study, we efficiently utilized Celloger® Pro's multi-positioning features and the user-friendly lens exchange capability to observe actin dynamics at high magnification.

Reference

1. Pier Paolo D'Avino., et al. "Cytokinesis in Animal Cells" Cold Spring Harbor Perspectives in Biology (2015): 7: a015834

2. J. W. SANGER., "The Use of Cytochalasin B to Distinguish Myoblasts from Fibroblasts in Cultures of Developing Chick Striated Muscle" Proceedings of the National Academy of Sciences of the United States of America Volume 71 no. 9 September (1974): 3621-3625.

3. YAHARA, ICHIRO., et al. "Correlation between Effects of 24 different cytochalasins on cellular structures and cellular events and those on actin in vitro" The journal of cell biology Volume 92 January (1982): 69-78.

4. Awtar Krishan., "Fine structure of cytochalasin-induced multinucleated cells" Journal of ultrastructure research Volume 36 July (1971): 191-204.

CURIOSIS

APPLICATION NOTE

Enhancing drug response evaluation through real-time monitoring of spheroid cytotoxicity

Using Celloger® Pro

■ Introduction

Cell culture systems are indispensable in the field of biomedical research, where 2D cultures are widely used because of their cost-efficiency and convenience. Nevertheless, the limitations of 2D culture systems, such as the loss of cell-to-cell or cell-to-matrix interactions and tissue-specific structures, hinder their capacity to mimic in vivo conditions, especially in disease models like cancer.[1] Due to these limitations, there is a growing interest in 3D culture systems that provide more realistic model resembling a complex in vivo environment. These 3D systems hold immense promise for monitoring crucial factors such as cytotoxicity, drug resistance, and cellular responses within the cancer microenvironment.[2,3] Moreover, they have significantly advanced drug safety and efficacy evaluations, facilitating early-stage drug discovery and development.[4]

The study presented herein highlights the power of Celloger® Pro, a cutting-edge live cell imaging system, in investigating the effects of an anticancer drug, Staurosporine, on 3D spheroids made from HEK293-GFP stable cells. This application note details the comprehensive results obtained using Celloger® Pro, demonstrating its capacity to dynamically capture and quantify cellular responses to drug treatment in a three-dimensional context.

■ Method

HEK293-GFP cells were seeded at 10,000 cells/well in a 96-well cell floater plate (SPL, 34896) which facilitates the formation of spheroid structure. Following overnight incubation, various concentrations of staurosporine (SSP) were treated: 0 μM (control), 0.1 μM, and 1 μM. Additionally, 4 μM of EthD-1 (Sigma, 46043), a fluorescent marker that selectively stains dead cells, was treated. Subsequently, real-time imaging was conducted using a Celloger® Pro. Images were captured at 30-minute intervals over 24 hours, with a 2X lens.

■ Result

To investigate the response of HEK293-GFP spheroids to the anti-cancer drug SSP, we monitored the real-time reduction in spheroid size using brightfield and green fluorescence imaging. Simultaneously, cell death was evaluated at different time points by measuring the intensity of red fluorescence. As the concentration of SSP increased, there was a corresponding rise in red fluorescence intensity, indicating signs of cell death. This trend became more pronounced over time (Fig. 1A). The relative red fluorescence intensity was quantified and graphically presented using Celloger® Pro's analysis software, which provided an insightful illustration of the spheroids' response to drug-induced cell death (Fig. 1D).

Additionally, the progression of cell death corresponded with a reduction in the spheroid's size, evidenced by the green fluorescence channel images. This clearly demonstrated the correlation between decreased spheroid size and intensified red fluorescence in the merged green and red fluorescence images, providing a direct visualization of the drug's impact on cellular viability (Fig. 1A). To further validate the decrease in spheroid size induced by SSP treatment, we precisely measured the spheroid's diameter using Celloger® Pro analysis software (Fig. 1B). The spheroid's size was quantified and effectively visualized through graphical representation, offering a clear and comprehensive depiction of the observed changes (Fig. 1C). These result underscores Celloger® Pro's capability to provide real-time insights into the dynamic changes occurring within 3D cellular structures.

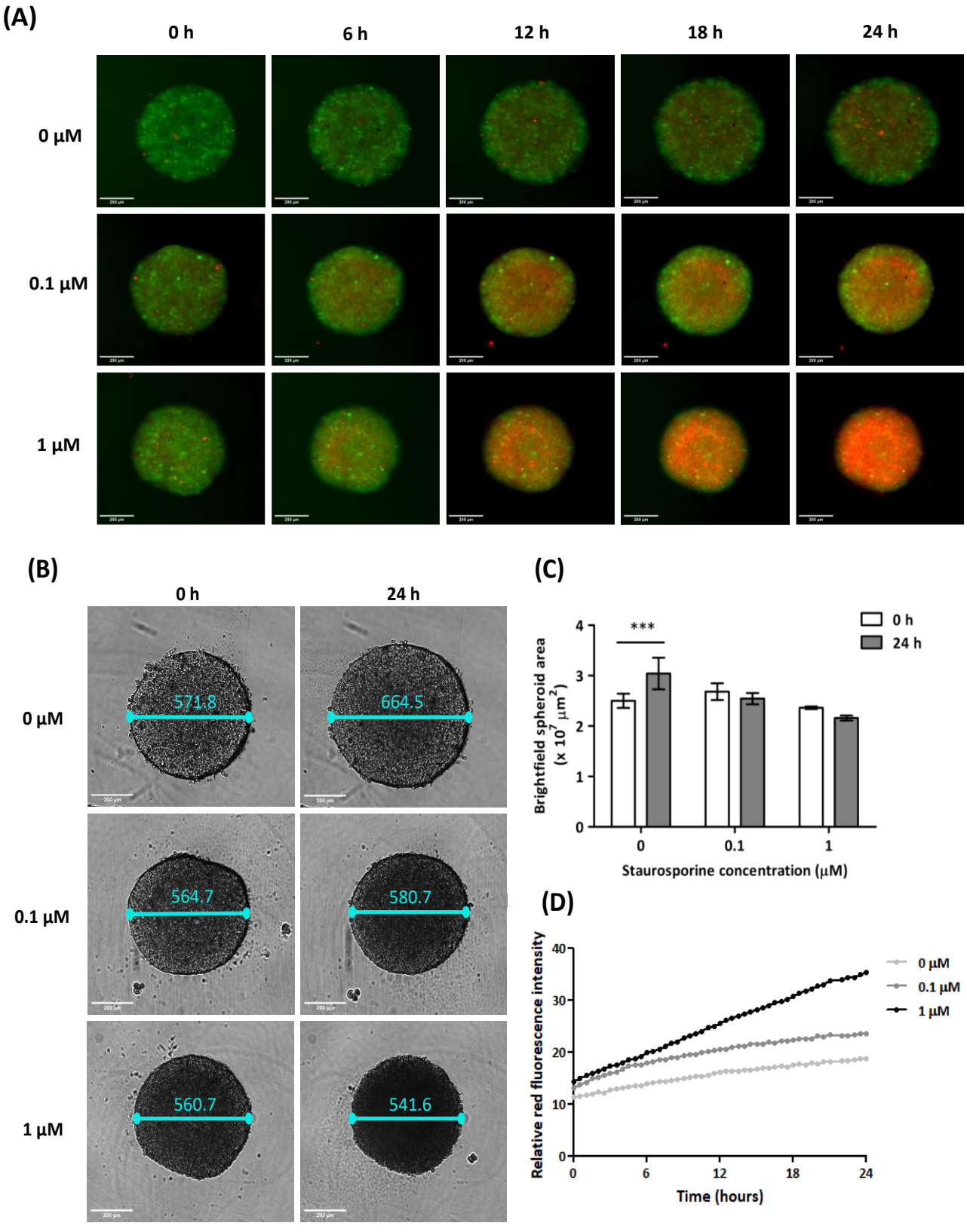

Figure 1. The results of spheroid cells with 0, 0.1, and 1 µM of SSP.

(A) Merged of green and red fluorescence images for each concentration of SSP (scale bar: 200 µm). (B) Brightfield images with spheroid's diameter (scale bar: 200 µm). (C) Comparative graph of spheroid area at 0 and 24 hours for each concentration of SSP. n=3 for each group. ***P < 0.0001 (D) Relative red fluorescence intensity graph over time.

■ Conclusion

The results presented in this application note exemplify the invaluable capabilities of Celloger® Pro in probing complex cellular phenomena. By dynamically tracking the size reduction of 3D spheroids under SSP treatment and quantifying fluorescence intensity changes in response to cell death markers, Celloger® Pro proves to be an indispensable tool for both qualitative and quantitative live cell imaging. By combining the power of 3D spheroid culture with the real-time imaging capabilities of the Celloger® Pro, we have finally demonstrated its potential to revolutionize drug response evaluation and contribute to the advancement of early-stage drug discovery. Researchers can utilize its features to unravel the subtleties of cellular responses to drug treatments in a three-dimensional context, leading to deeper insights and accelerated advancements in anticancer research and beyond.

Reference

1. Fang, Ye, and Richard M. Eglen. "Three-dimensional cell cultures in drug discovery and development." Slas discovery: Advancing Life Sciences R&D 22.5 (2017): 456-472.

2. Ravi, Maddaly, et al. "3D cell culture systems: advantages and applications." Journal of cellular physiology 230.1 (2015): 16-26.

3. Baek, NamHuk, et al. "Real-time monitoring of cisplatin cytotoxicity on three-dimensional spheroid tumor cells." Drug design, development and therapy (2016): 2155-2165.

4. Huang, Zhaoming, Panpan Yu, and Jianhui Tang. "Characterization of triple-negative breast cancer MDA-MB-231 cell spheroid model." OncoTargets and therapy (2020): 5395-5405.

CURIOSIS

APPLICATION NOTE

Zebrafish observation using the Z stacking function

Using Celloger® Mini Plus

Zebrafish, along with mice, is a well-known animal model widely used in biological research such as epigenetics1, clinical research2, neuroscience research3 and so on. Mainly, this is because it is easy to manipulate the zebrafish embryos and larvae genetically, and they are easy to observe using an optical microscope since they are small in size and have high optical clarity.

We introduce the Celloger® series' functions for observing zebrafish. Celloger® Mini Plus provides a Z-stacking function that automatically generates multi-layer images and the Celloger® analysis software offers a merge function to combine the multi-layered fluorescent images easily. These functions enable researchers to observe three-dimensional (3D) structures in a single image. We observed transgenic zebrafish (larvae) expressing green fluorescent protein (GFP) using these functions, as detailed in steps 1 and 2 below.

■ Step1. Z-stacking

The 3D structures, such as tissue composed of cells, provide various information depending on the focal point; it is crucial to identify various focal points. By setting the distance between layers ("step") and the number of images taken ("N, N'"), Celloger® generates multi-layer images at regular intervals ("step") above and below the set position (Z position) (Figure 1). Different settings can be entered for each point, and different Z-stacking can be performed at various points.

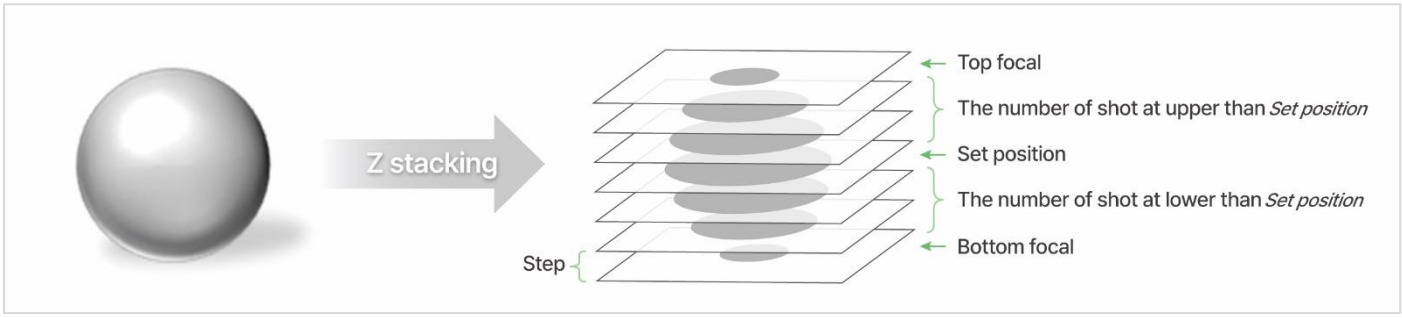

Figure 1. Z stacking

We utilized Celloger® Mini Plus, which enables fluorescence imaging, to create Z-stacked images of the fluorescent transgenic zebrafish. Because the acceptable focus plane varies for each part of the three-dimensional larva, we verified the appropriate focal planes by manipulating the motorized Z stage of the process. We identified the top (Z = 4.585) and bottom (Z = 4.685) focal planes among several focal planes and the coordinate (Z = 4.635) was set corresponding to the middle as the scan position. In addition, we set to take five pictures at 10 μm intervals above and below the scan position as the center (Figure 2). Figure 3 shows the pictures captured from the top, middle, and bottom focal planes of the zebrafish. In the side view, the shape of the head was definite in the bottom focal plane, while the ventral part was clearly visible in the top focal plane.

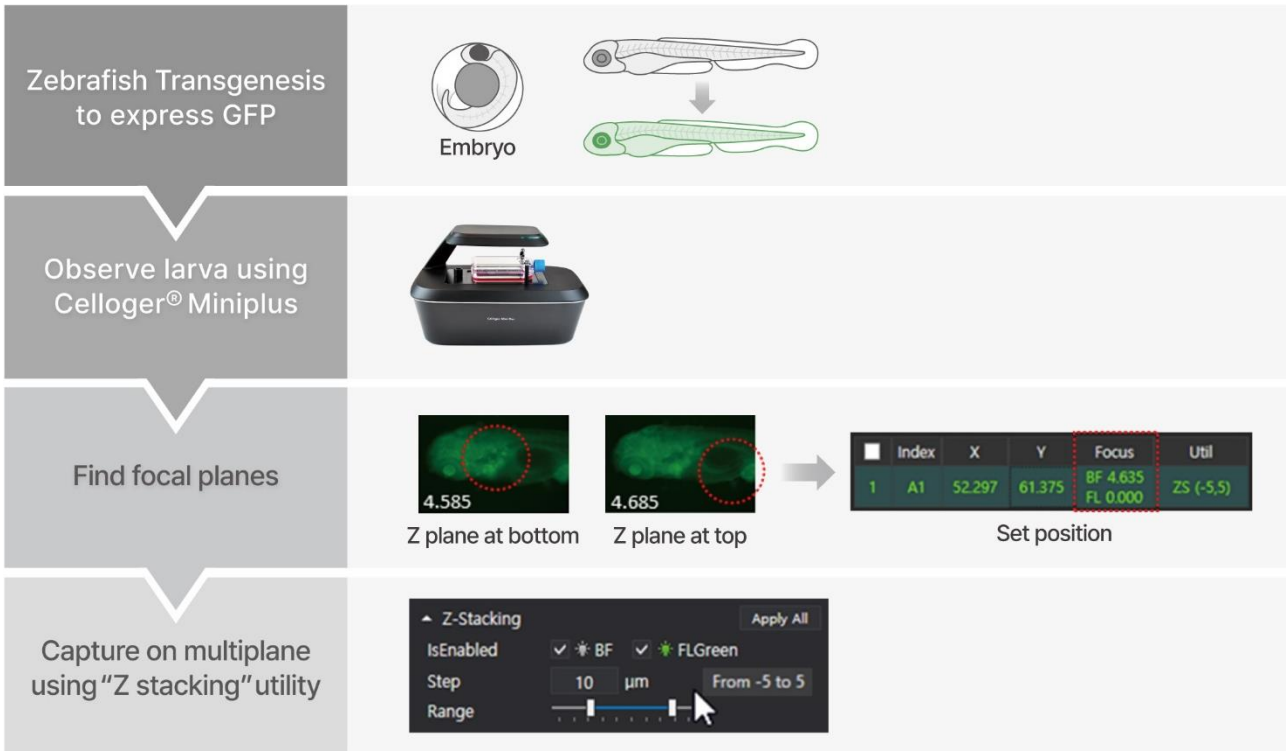

Figure 2. Procedure

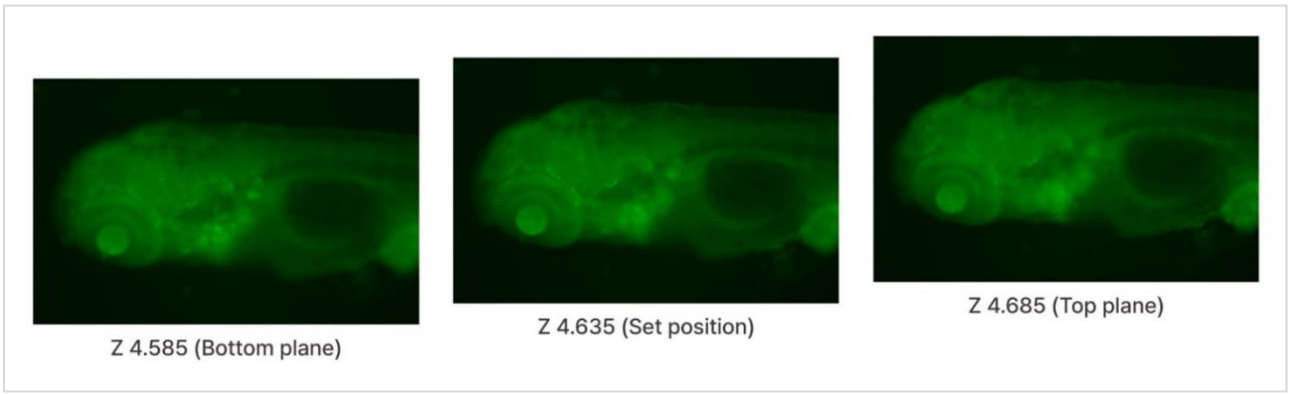

Figure 3. Result

■ Step2. Z-projection

Multi-layer imaging (Z-stacking) is essential for observing the 3D model. However, interpreting the results of multiple images obtained by multi-layer imaging is laborious and time-consuming. The Z-projection function, which merges several layers into one image, allows one 3D sample to be observed at a glance as one image, thereby increasing the researcher's insight.

Projection type is a method of integrating several Z coordinates located at each X-Y position. The "maximum" is used to integrate the brightest pixel among several Z coordinate points, while the "average" is used to calculate the average brightness of several Z coordinate points (Figure 1). In addition, "add deviation value," an element that can be reinforced, was added to the Celloger® analysis software to obtain a clearer image.

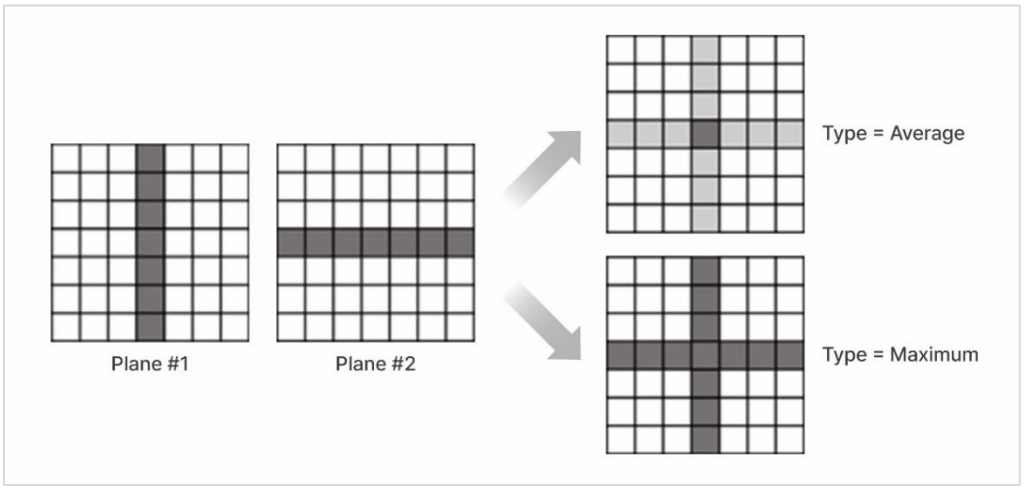

Figure 1. Explanation of Z projection type

If the images taken with Z-stacking are opened in the Celloger® analysis software, and the "merge" button on the Z-stack tab is clicked, a Z-projection image can be obtained (Figure 2). The appropriate projection type differs among samples; confirming the result for each type is recommended. Figure 3 shows the result of stitching three images for projection by selecting the "maximum" type and "add deviation value" option. The head structure is clearly expressed on the bottom focal plane, and the unique ventral shape, which can be observed on the top focal plane, is expressed as a single image using the projection function.

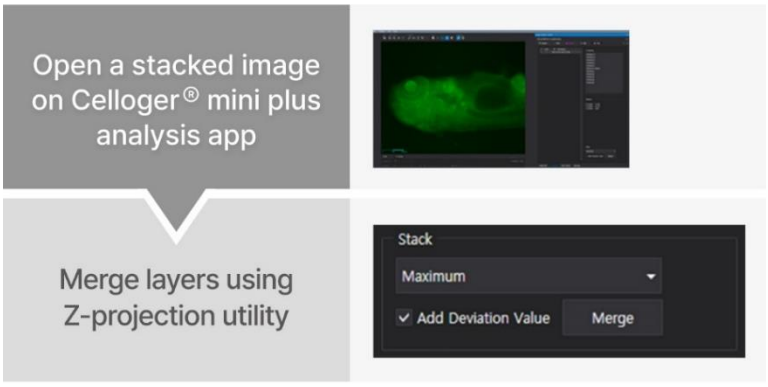

Figure 2. Procedure

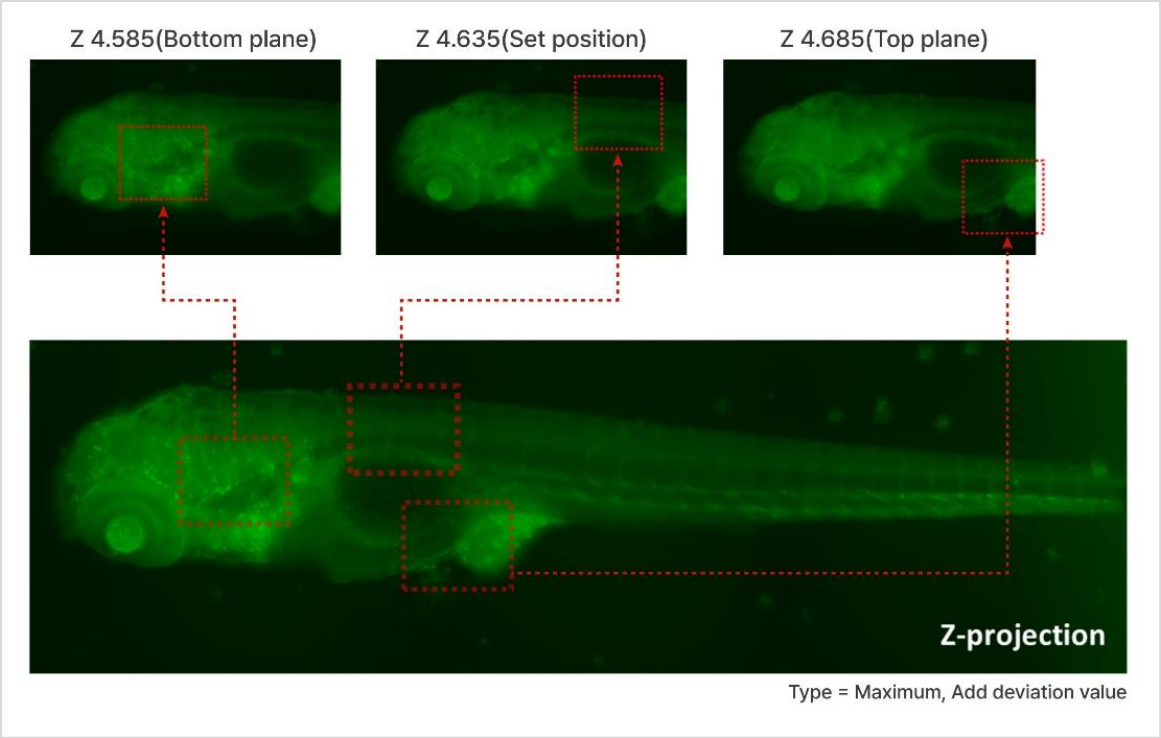

Figure 3. Result

■ Conclusion

We have successfully acquired high-quality fluorescence images of Zebrafish using the Celloger® Mini Plus system. The three-dimensional structure's multiple layers of information were successfully combined and expressed in a single image with clarity. This experiment confirms the feasibility of capturing 3D images using various other sample types, including spheroids and organoids which could expand the range of research scope available to researchers.

Reference

1. Balasubramanian, S., Raghunath, A., & Perumal, E. (2019). Role of epigenetics in zebrafish development. Gene, 718, 144049. https://doi.org/10.1016/j.gene.2019.144049

2. Kinth, P., Mahesh, G., & Panwar, Y. (2013). Mapping of zebrafish research: a global outlook. Zebrafish, 10(4), 510–517. https://doi.org/10.1089/zeb.2012.0854

3. Stewart, A. M., Braubach, O., Spitsbergen, J., Gerlai, R., & Kalueff, A. V. (2014). Zebrafish models for translational neuroscience research: from tank to bedside. *Trends in neurosciences, 37(5),* 264-278.

CURIOSIS

APPLICATION NOTE

Analysis of Nocodazole-induced Cytotoxicity using Celloger® Mini Plus

1. Introduction

Cytotoxicity refers to the degree of damage to cells caused by chemical substances or physical factors. Measuring it through cytotoxicity assay is essential for drug development and biological research. Cells undergo complex signaling pathways that causes various cell death processes such as apoptosis, necrosis, and necroptosis. However, most cytotoxicity assays are measured at the end-point that makes it difficult to study the dynamic response of cells to drugs.

In this application note, we aimed to examine the performance of a cytotoxicity assay using real-time imaging. Cells treated with various concentrations of Nocodazole, the anti-cancer drug, were stained with fluorescent dye during cell death, then monitored with **Celloger® Mini Plus**. It was observed through time-lapse imaging that apoptosis increased in a Nocodazole dose-dependent manner, and the degree of apoptosis was quantitatively measured and graphed using the Analysis software provided with the **Celloger® Mini Plus**.

2. Method

HeLa cells were counted using Facscope B (Curiosis Inc.), an automatic cell counter and seeded at 1 x 10^4 cells/well in a 48 well plate. After culturing overnight, cells were treated with various concentrations (16.625 nM, 31.25 nM, 62.5 nM, 125 nM, 250 nM) of Nocodazole. At this point, CellTox green dye (Promega, G8742) which binds to DNA of cells with impaired membrane integrity during cell death was added to the sample. Using Celloger® Mini Plus installed inside an incubator, cell images were acquired every 1 hour for 48 hours then the images were analyzed using the Analysis software. The cell death rate (%) was calculated as *fluorescence coverage (= dead cell) ÷ bright field confluency (= total cell)*.

3. Result

As a result of treating the cells with nocodazole by different concentrations and imaging them over time, the morphology of cells changed in a concentration-dependent manner and the confluency shrinkage was observed in bright field imaging (Figure 1A, B). In addition, fluorescence imaging of dead cells stained by CellTox dye, measuring its coverage and quantifying the cell death showed that the proportion of fluorescent cells increases with apoptosis (Figure 1C).

Figure 1. Analysis of Nocodazole dose-dependent cell death using time-lapse imaging

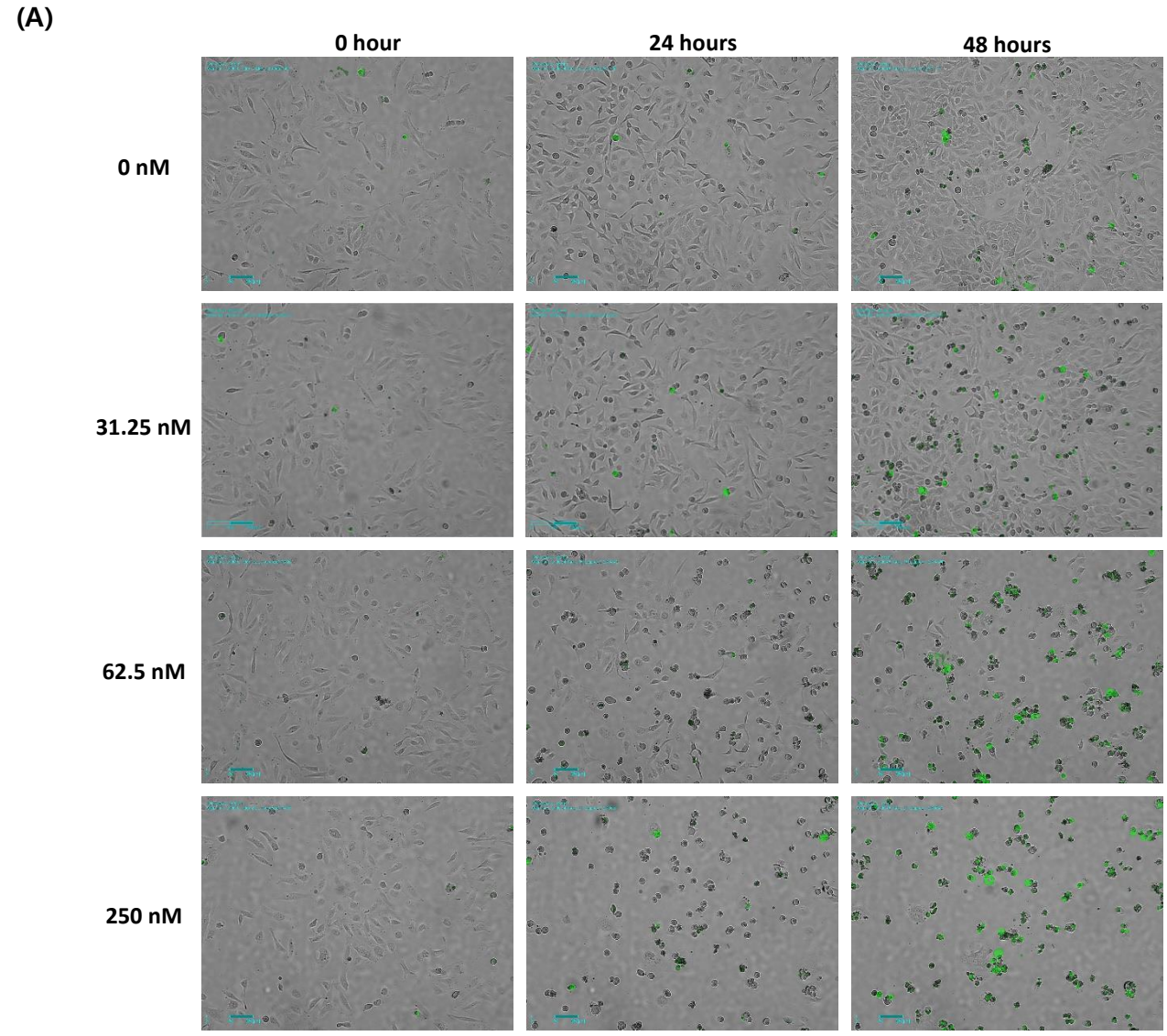

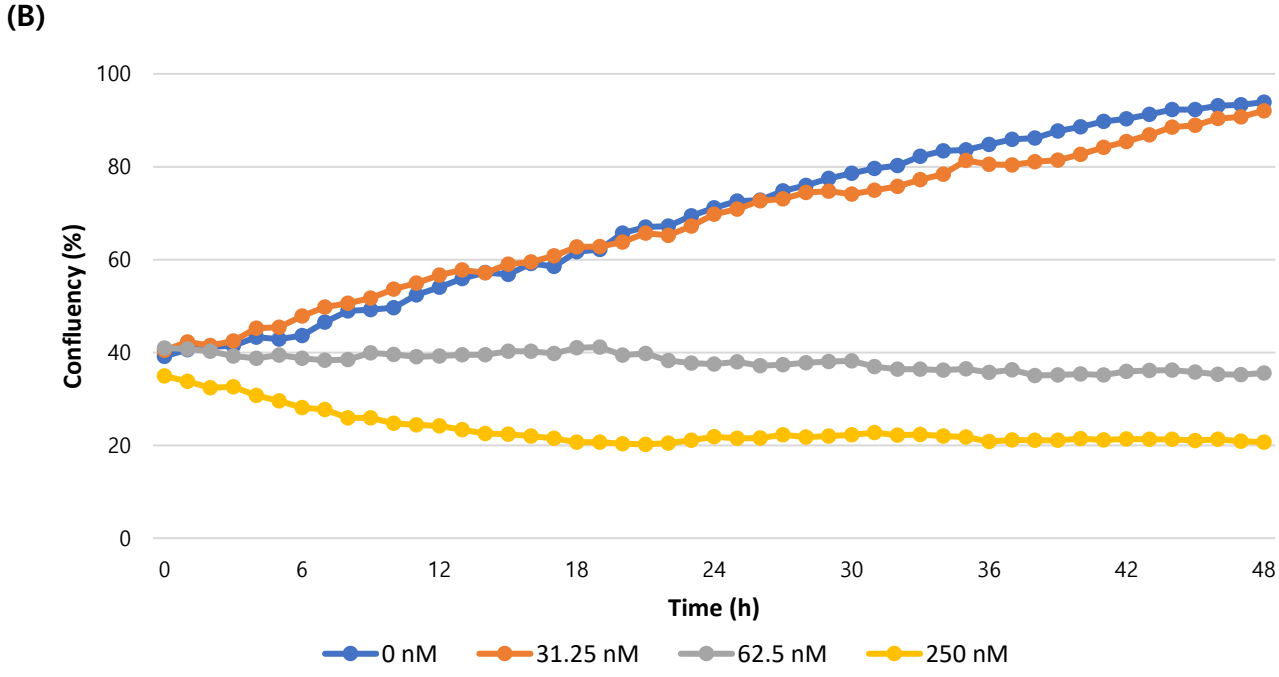

(C)

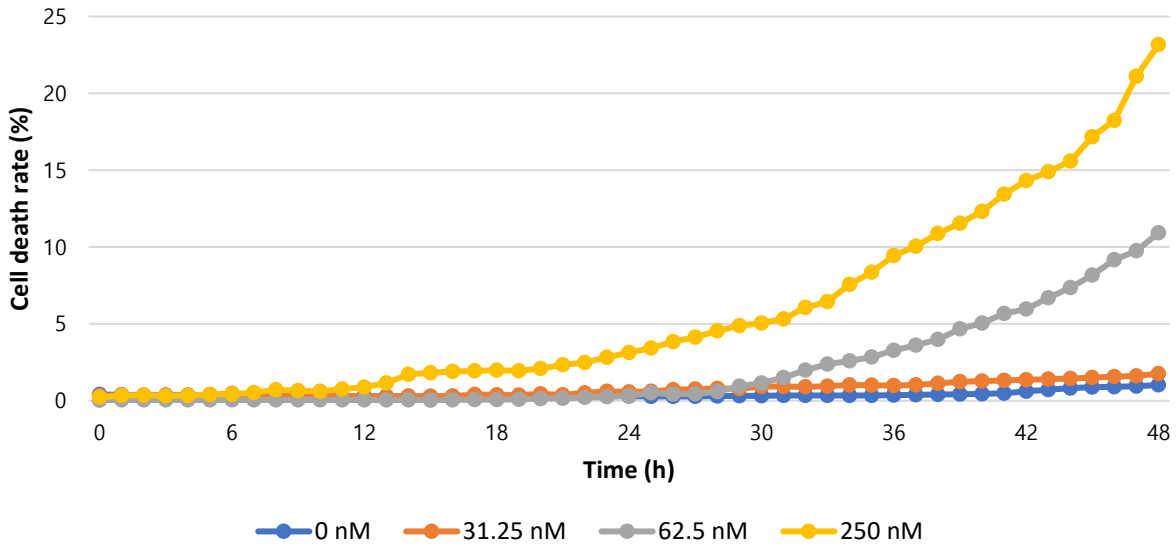

(A) *Merged bright field and fluorescence images for each concentration of Nocodazole. The images are shown at 24-hour intervals, and green fluorescence indicates the dead cells. (Scale bar: 200 um)*
(B) *The confluency (%) graph of total cell over time.*
(C) *The graph of cell death rate (%) over time.*

4. Conclusion

Celloger® Mini Plus is a live cell imaging device that can simultaneously perform bright field and fluorescence imaging in an incubator. The system has a fully motorized camera that enables imaging of various positions at a set interval programmed by the user. The confluency graph over time can be acquired by calculating the confluency of captured images using the Analysis software. Furthermore, by measuring the fluorescence coverage, the degree of apoptosis according to the concentration of Nocodazole can be quantified.

CURIOSIS

APPLICATION NOTE

Observation of Mitosis Using Celloger® Mini plus

1. Introduction

In the process of 'cell cycle', cells grow and divide into two genetically identical daughter cells. It is regulated by a complex signaling pathway which keeps cell homeostasis by regulating cell division and DNA duplication[1]. On the other hand, because cancer cells grow and divide indefinitely out of cell cycle control, anti-mitotic drugs are used to suppress abnormal proliferation of cancer cells[2]. In particular, Nocodazole is known to be a representative anti-mitotic drug for cancer treatment, and it has the characteristics of disturbing microtubule dynamics during cytoplasmic and nuclear division[3,4].

In the present study, we examined the anti-mitotic activity of nocodazole against cancer cell line by monitoring the cell division process. To this end, Hela cells were stably transfected with green fluorescent protein fused histone 2B (H2B-GFP), which visualizes the dynamics of chromosomal structure during cell cycle progression[5]. And then, the cell division was monitored in real time after treating the cell with or without nocodazole using **Celloger® Mini Plus**, a live cell imaging device.

2. Method

HeLa cells transfected with H2B-GFP plasmid were seeded into a 24 well plate at 4 x 10^4 cells/well. Cells were cultured with 10% Fetal bovine serum and Dulbecco's Modified Eagle's Medium to which 300 ug/mL G418 was added. After overnight culture to attach the cells, they were incubated with or without 62.5 nM of nocodazole, and real time imaging was conducted using **Celloger® Mini Plus** (Bright field & green fluorescence channel, 10X optics). Images were taken every 15 minutes for 24 hours.

3. Result

Brightfield and fluorescence time-lapse imaging of Hela cells transfected with green fluorescent protein fused H2B was performed to observe nuclear changes in mitosis. In the bright field image, the nuclear membrane was clearly visible at the beginning, then they gradually disappeared and metaphase where chromosomes were aligned at the center of the cell was observed in both the bright field and fluorescence images (Figure 1A). At this point, chromosomes were condensed, and fluorescence became more intense compared to the previous stage. Chromosomes that entered the

later stage were separated into two sister chromatids and each one moved to opposite poles of the cell. And as shown in the last image, two daughter cells were finally generated in telophase. On the contrary, in the cells treated with nocodazole, the cell division process did not proceed any further as the chromatids could not be divided into both ends. In the bright field image, the cells continued to not adhere to the bottom anymore, and it was confirmed that the DNA was eventually fragmented, which resulted in apoptosis in the fluorescence image (Figure 1B).

Figure 1. Timelapse images of H2B-GFP transfected Hela cells with or without nocodazole.

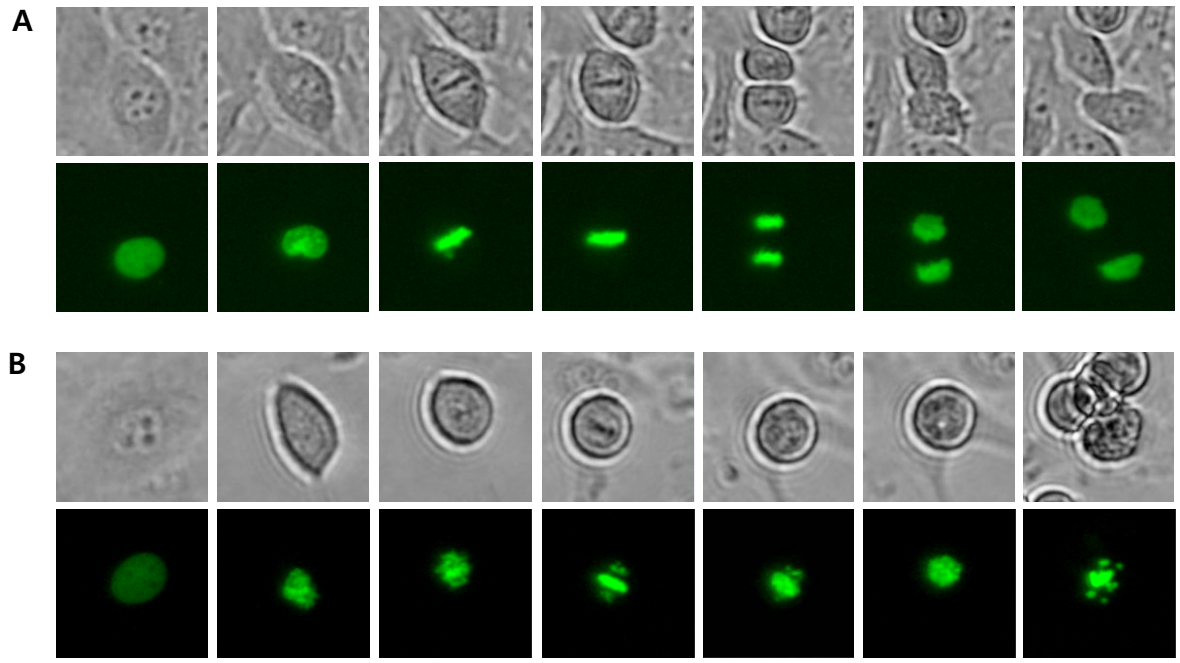

In each panel, upper images are brightfield images and lower images are fluorescence images. Image J program was used for cropping and correction.

(A) *Control cells were not treated with nocodazole*.

(B) *Cells were treated with 62.5 nM nocodazole.*

4. Conclusion

Fluorescent labeling is a useful tool to observe the dynamics of organelles in live cells. So far, plasmids have been developed to observe various organelles or target protein using fluorescent fusion protein, and many studies have been conducted to verify the changes in organelles or protein translocation induced by various stimulations.

In this application note, we performed a nuclear labeling method using histone and green fluorescence fusion protein that binds to DNA. To confirm the effect of nocodazole on cell division, cells were monitored over time and images were acquired using **Celloger® Mini Plus**, a real-time live cell imaging device. The system has a fully motorized camera that enables imaging of various positions at a set interval programmed by the user. This makes it possible to track changes in each cell under different conditions.

5. Reference

1. Mills, Christopher C., E. A. Kolb, and Valerie B. Sampson. "Development of Chemotherapy with Cell-Cycle Inhibitors for Adult and Pediatric Cancer Therapy Combination Therapies for Cancer." *Cancer research* 78.2 (2018): 320-325.

2. Otto, Tobias, and Piotr Sicinski. "Cell cycle proteins as promising targets in cancer therapy." *Nature Reviews Cancer* 17.2 (2017): 93-115.

3. Blagosklonny, Mikhail V. "The power of chemotherapeutic engineering: arresting cell cycle and suppressing senescence to protect from mitotic inhibitors." *Cell cycle* 10.14 (2011): 2295-2298.4. Taciak, Bartłomiej, et al. (2018) *PloS one*

4. Endo, Kingo, et al. "Nocodazole induces mitotic cell death with apoptotic-like features in Saccharomyces cerevisiae." FEBS letters 584.11 (2010): 2387-2392.

5. Anda, Teru, Kevin F. Sullivan, and Geoffrey M. Wahl. "Histone–GFP fusion protein enables sensitive analysis of chromosome dynamics in living mammalian cells." *Current Biology* 8.7 (1998): 377-385.

CURIOSIS

APPLICATION NOTE

An integrated live cell monitoring system for stable imaging of suspension cells in immunological research

Using Celloger Mini Plus to observe morphological changes and phagocytic activity in macrophage cell line

As white blood cells responsible for immune function are suspension cells that travel along blood vessels, immunology studies often use various suspension cell lines originating from white blood cells. Dealing with suspension cells, unlike adherent cells, slight movement of a plate when locating it on the microscope causes the cells to float. Aside from the problems caused by temperature and CO_2 instability, it is in fact not possible to use a traditional microscope to monitor cells in real time. Therefore, in order to stably monitor suspension cells, a live cell imaging device such as **Celloger** that operates inside an incubator is essential[1]. In addition, with **Celloger Mini Plus,** the camera inside the system moves to capture the images of cells in multiple positions to keep the cell sample in a steady state instead of having a movable stage with a plate on it. When the suspension cells were monitored both by **Celloger** and microscope, imaging with **Celloger** was more stable compared to using a microscope in which several cells were out of focus (Figure 1).

*For suspension cell imaging using an inverted microscope, cell fluctuation is inevitable since the sample must be taken out of an incubator, placed on the microscope stage, and be moved to locate other positions within the plate. In this process, many cells are observed to be floating off the floor and are out of focus (Left image). On the other hand, imaging with **Celloger Mini Plus** enables the entire process of imaging inside an incubator. The plate is stably fixed on the device and multiple positions within the plate can be imaged by moving the camera inside the system; thus nothing causes cell floating and no cells are observed to be out of focus (Right image).*

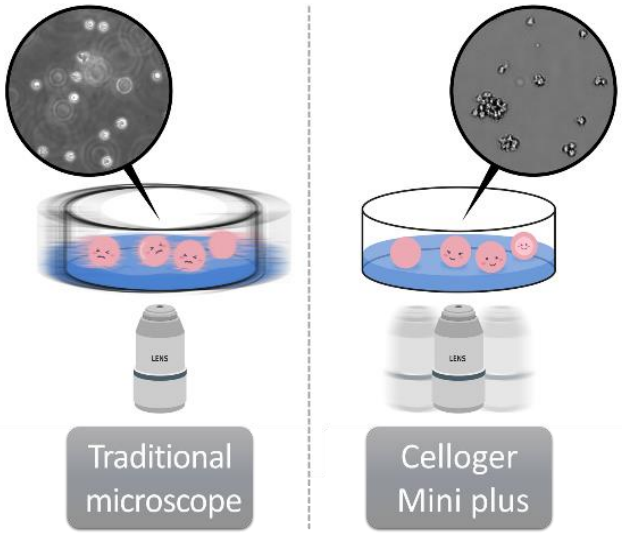

Figure 1. Advantages of using Celloger during suspension cell imaging

White blood cells as a part of the immune system fight infection and defend the body against foreign materials. A first line of defense system known as innate immunity generates fast inflammatory responses to immediately prevent the spread and movement of foreign pathogens throughout the body. Because activation of the innate immune system is initiated within hours and generates rapid inflammatory responses, it is important to monitor the various cellular defenses occurring in this process in real time. An important function of innate immunity is the rapid recruitment of immune cells to an infected area. Among white blood cells, monocytes infiltrate tissues and differentiate into macrophages, while inducing an immune response against invading pathogens through phagocytosis. We performed live cell imaging with **Celloger Mini Plus** (Bright field & green fluorescence channels, 10X objective) using the Raw264.7 cell line, which represents the functional characteristics of macrophage and is well known for changes caused by lipopolysaccharide (LPS)[2].

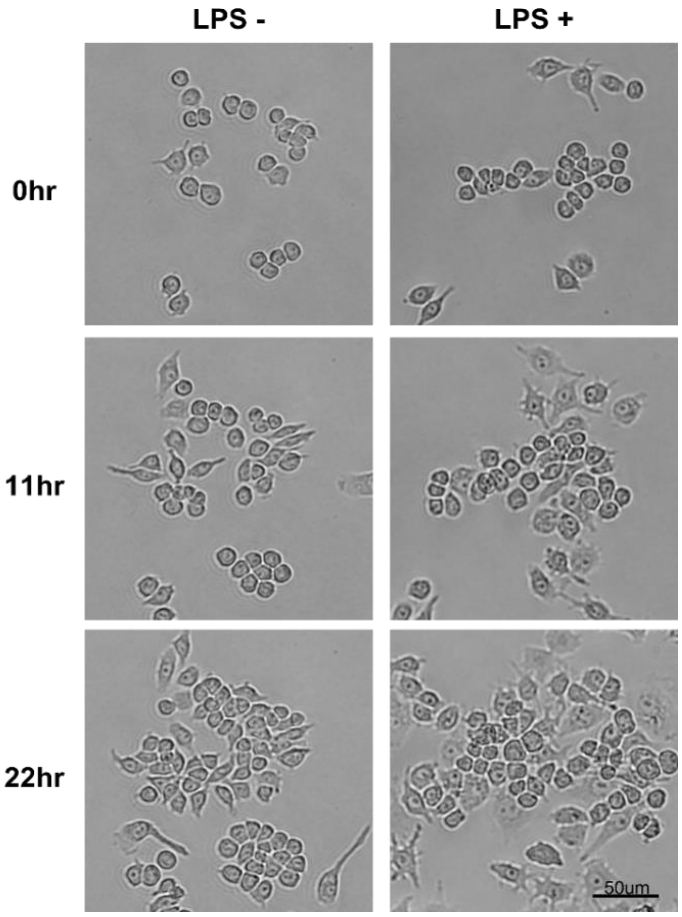

Figure 2. Monitoring morphological changes in Raw264.7 cells with LPS

When Raw264.7 cells were stimulated by LPS, the differentiated cells increased. As round and thick cuboidal cells in a loosely adhered state were differentiated, they slowly spread and adhered more firmly in a spindle form, and this was observed through images taken every 15 minutes by ***Celloger Mini Plus*** *(10X optics).*

According to the study by Saxena et al. (2003), Raw264.7 cells stimulated by LPS differentiate into dendritic-like cells[3]. We confirmed through real-time monitoring using **Celloger Mini Plus** that the cells adhered more firmly and became wider and flatter than the cells without LPS treatment (Figure 2).

This change in the morphology was more visible 11 hours after LPS treatment and lasted for up to 22 hours. Also, LPS stimulation resulted in cell proliferation, which was quantified through **Celloger**'s confluency analysis function (Figure 3).

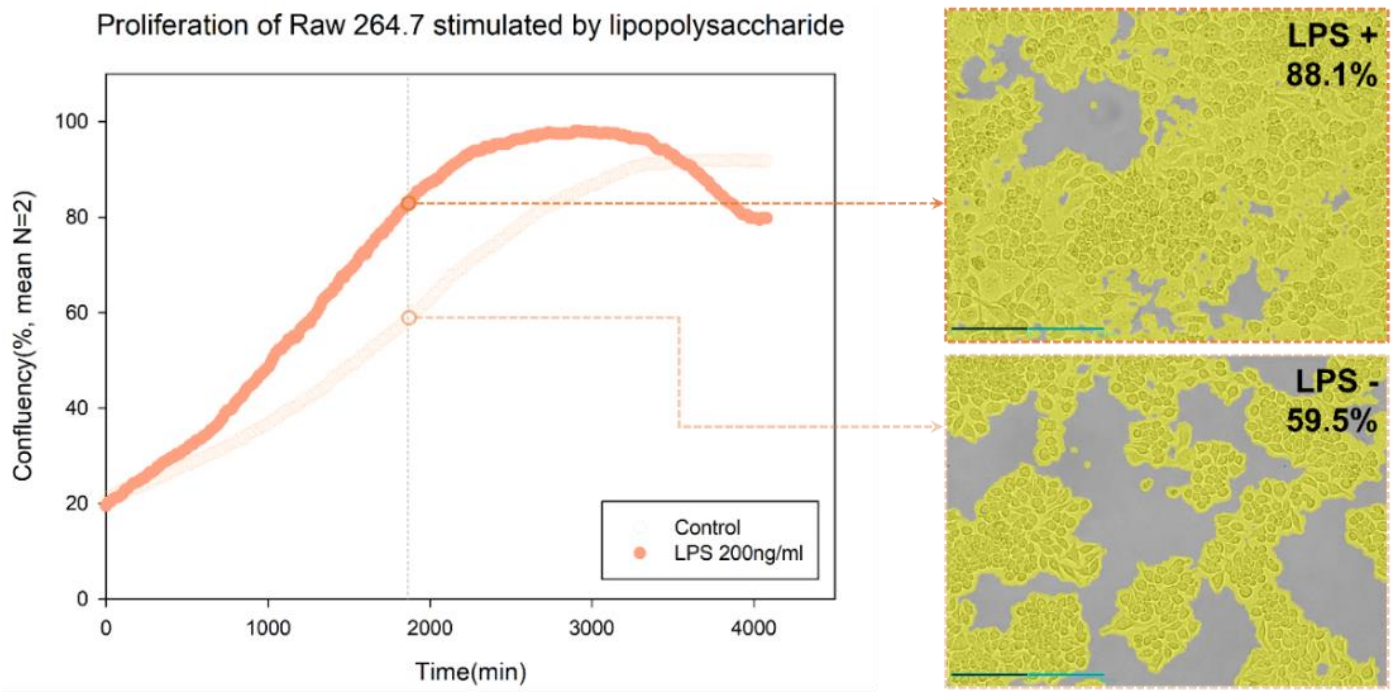

Figure 3. Growth curve of LPS-stimulated cells through confluency analysis

*By using the time-lapse images (captured via **Celloger Mini Plus,** 10X optics) and analyzing the cell confluency with the **Celloger Mini Plus** analysis app, a cell growth graph can be obtained.*

There is a report that LPS-induced activation of macrophage increases phagocytosis through the toll-like receptor 4-dependent pathway[2,4]. To confirm this in real time, we performed fluorescence imaging using fluorescent latex beads that were engulfed by macrophages. The 2um-sized fluorescence beads swayed easily with the slightest movement and floated above the plate. This not only decreases the bead uptake efficiency of cells but can also make imaging difficult. In fact, even commercially available phagocytosis assay kits recommend only counting bead-engulfed cells by fluorescence microscopy or flow cytometry after properly washing at the endpoint to remove non-engulfed beads[5,6]. In this experiment, **Celloger**'s real-time imaging showed the entire bead phagocytosis process of the cells and the bead engulfment taking place only for the activated cells that were spread flat with LPS stimulation (Figure 4A).

The way these activated cells behave are expected to be possible because they efficiently move toward the beads in a spindle shape that cause directional migration compared to the round and cube-like shape before differentiation. It was also observed in real time that the beads were divided into daughter cells along with the cytoplasm when the cells were divided after bead uptake (Figure 4B).

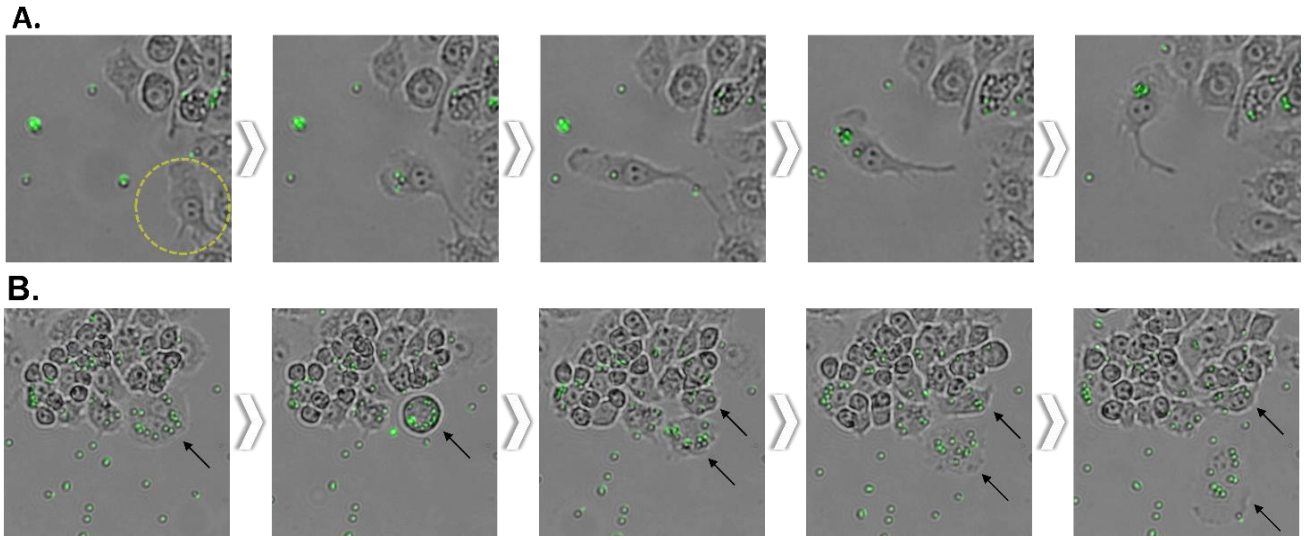

Figure 4. Phagocytosis of LPS-stimulated Raw264.7 cell observed with Celloger Mini Plus (Bright field & green fluorescence channel, 10X optics)

A. *It was observed that the activated Raw264.7 cells after LPS stimulation engulfed the fluorescent bead. Time-lapse images were taken at a 15-minutes interval to observe cells migrate toward the bead and uptake the bead.*

B. *The engulfed beads inside the cells are divided into daughter cells along with the cytoplasm during mitosis.*

In addition, it is possible to obtain dynamic process information for various molecular environments by using the unique characteristics of the fluorescent probe. If a fluorescent dye can be additionally imaged along with the bright field imaging, it can be used for further in-depth studies. Using cell-impermeant nucleic acid stain, cytotoxicity can be evaluated through the increase in the permeability of the dye due to membrane damage during apoptosis[7]. And in the case of neutrophil in particular, NET formation can also be detected by nucleic acid staining[8]. Furthermore, it is possible to quantify the generation of reactive oxygen species[9] in cells using dyes that react with reactive oxygen species or observe the intracellular acidification in the process of endocytosis and phagocytosis using pH-sensitive dye[10].

Live cell imaging with **Celloger Mini Plus** enables obtaining high-resolution images of cells while eliminating physical disturbances such as cell damage or shaking. It is an automated system that functions perfectly inside an incubator, eradicating the need to move the device in and out of the incubator. Unlike other devices, **Celloger Mini Plus** doesn't have a movable stage but instead, the camera inside the system moves to capture the images of cells in multiple positions. Since the vessel and cell samples are in a steady state, this provides a stable environment for the cells to grow and increases the success rate of cell-based research. Various types of culture vessels are compatible with the system, and it has high position reproducibility for stable scanning performance during multi-point imaging; therefore, **Celloger Mini Plus** will bring reliable results in immunology research.

Reference

1. Awasthi, Bhuwan Prasad, et al. (2021) *Journal of Enzyme Inhibition and Medicinal Chemistry*

2. Wu, Tsu-Tuan et al. (2009) *Toxicology letters* vol.

3. Saxena, Rajiv K et al. (2003) *Journal of biosciences* vol.

4. Taciak, Bartłomiej, et al. (2018) *PloS one*

5. Ariganello, Marianne B., et al. (2018) *International journal of nanomedicine*

6. Manda-Handzlik, Aneta, et al. (2018) *Immunology and Cell Biology*

7. Riss, Terry, et al. (2019) *Assay Guidance Manual* [internet]

8. Takishita, Yutaka, et al. (2019) *Journal of Clinical Biochemistry and Nutrition*

9. Pal, Kunal, et al. (2019) *Materials Science and Engineering: C*

10. Diwu, Zhenjun, et al. (1999) *Chemistry & biology*